

Full Title: An Efficient, Chemically-Defined Semisynthetic Lipid-Adjuvanted Nanoparticulate Vaccine Development System

Short Title: Semisynthetic Lipid-Adjuvanted Vaccine Development

Authors and Academic Degrees:

Peter M. Moyle^{a,b} – BPharm(Hons), PhD

Jon Hartas^c – BSc

Anna Henningham^a – BBiotech(Hons), PhD

Michael R. Batzloff^c – BSc(Hons), PhD

Michael F. Good^c – BSc, MBBS, PhD, MD, DSc

Istvan Toth^{a,b,d} – BSc, PhD, CSc, DSc

Affiliations:

^a School of Chemistry and Molecular Biosciences, The University of Queensland, St Lucia 4072, QLD, AUSTRALIA

^b Institute for Molecular Biosciences, The University of Queensland, St Lucia 4072, QLD, AUSTRALIA

^c Institute for Glycomics, Griffith University, Southport 4222, QLD, AUSTRALIA

^d School of Pharmacy, the University of Queensland, Woolloongabba 4102, QLD, AUSTRALIA

Corresponding Author/s:

Dr. Peter Moyle

School of Chemistry and Molecular Biosciences

Building 68

The University of Queensland, St Lucia 4072, QLD, AUSTRALIA

Email: p.moyle@uq.edu.au

Telephone: +61 (7) 3346 9893

Prof. Istvan Toth

School of Chemistry and Molecular Biosciences

Building 68

The University of Queensland, St Lucia 4072, QLD, AUSTRALIA

Fax: +61 (7) 3365 4273

Email: i.toth@uq.edu.au

Telephone: +61 (7) 3346 9892

Conflict of Interest Statement: None of the authors has declared a conflict of interest which may arise from being named as an author on the manuscript.

Sources of Support for Research:

This work was supported by an Australian National Health & Medical Research Council (NHMRC) program grant (496600). P.M.M. was funded by the American Australian Association and an NHMRC postdoctoral training fellowship (569869). I.T. is funded by an Australian Research Council (ARC) Australian Professorial Fellowship (DP110100212).

Word Count (Abstract): 150

Word Count (Manuscript): 4438

No. Figures/Tables: 5 Figures/0 Tables

No. References: 43

Abstract:

A novel vaccine development platform that enables the site-specific conjugation of synthetic lipid adjuvants to recombinant proteins was produced. This technology facilitates the simple and efficient production of homogeneous, chemically-defined, semisynthetic lipoprotein vaccines. Using a polytope 'string-of-beads' approach, a synthetic gene incorporating seven *Streptococcus pyogenes* M protein strain-specific antigens, and a conserved M protein antigen (J14) was produced, expressed, and attached to a lipoamino acid based adjuvant (lipid core peptide; LCP). Nanoparticles (40 nm diameter) of an optimal size for stimulating antibody-mediated immunity were formed upon the addition of these lipoproteins to aqueous buffer (PBS). Systemic antigen-specific IgG antibodies were raised against all eight antigens in C57BL/6J mice, without the need to formulate with additional adjuvant. These antibodies bound cell surface M proteins of *S. pyogenes* strains represented within the polytope sequence, with higher antibody levels observed where a dendritic cell targeting peptide (DCpep) was incorporated within the LCP adjuvant.

Key words: Lipid adjuvants; Subunit vaccines; Recombinant proteins; Semisynthesis; *Streptococcus pyogenes*

Background

Immunization with attenuated microorganisms has proven to be one of the most effective means to prevent disease.¹ Despite this success, many diseases lack effective vaccines (e.g. rheumatic heart disease (RHD), malaria, and tuberculosis),² in part because of significant risks associated with this approach (e.g. infectivity in

immunocompromized individuals). This has led to a shift towards subunit vaccines, which contain only the minimal components required to elicit protective immunity.¹ While this approach enhances vaccine safety, the capacity to elicit potent immune responses is significantly reduced, requiring their administration with powerful immunostimulatory compounds known as adjuvants.

A variety of molecules (lipids, glycolipids, nucleotides, and flagellin) have been investigated as adjuvants for subunit vaccines.³ Our work has focused on synthetic lipoamino acids⁴ (α -amino acids with variable length alkyl side-chains; Figure 1, A) as an alternative to bacterial or synthetic lipopeptide adjuvants (e.g. Pam2- and Pam3Cys) for peptide-based vaccines, due to their simple, inexpensive synthesis, and ability to be incorporated using standard peptide coupling protocols. The attachment of 2-3 lipoamino acids, with optimized side-chain length and spacing (e.g. Figure 1, A; called lipid core peptides (LCPs)), has been demonstrated to provide adjuvant activity towards a variety of peptide antigens,⁵ leading to antibody-mediated (mucosal and systemic)⁶ and cellular immunity⁷ following parenteral or mucosal administration.⁸ This adjuvant activity at least partially involves signaling through Toll-like receptor 2 (TLR2),⁹ through which bacterial lipopeptides also signal.³

In order to develop the aforementioned lipopeptide vaccines, protective peptide epitopes must be mapped for the disease of interest.¹⁰ In many cases this information is not available, or mapping experiments have failed to define linear protective epitopes, necessitating a whole protein approach. In addition, the ability to produce large amounts of synthetic homogeneous peptides, in high yield, rapidly decreases with increasing peptide length.¹¹ As a consequence, peptide vaccines can only incorporate a

few epitopes, reducing their capacity to protect whole populations against infection. A recombinant protein approach would overcome these difficulties, as proteins can be expressed on an industrial scale, with excellent batch-to-batch reproducibility, at lower cost than synthetic peptides,¹² and may incorporate a large number of antigens, with correct presentation of folded epitopes.

Based on this knowledge, we sought to develop techniques to produce semisynthetic LCP vaccines incorporating recombinant protein antigens (Figure 1, A). This approach allows the incorporation of non-natural components, linkages, and attachment configurations (e.g. branching), which could not be achieved with a recombinant approach alone, while generating a product that can be characterized at the molecular level. Further, the products of this approach crosslink antigen and adjuvant into the same molecule, ensuring their co-delivery to cells of the immune system, an approach that in many cases significantly enhances the immune response towards attached antigens.¹³ Maleimide conjugation was selected for this purpose as maleimides can be readily incorporated into our lipid adjuvants, are inexpensive to synthesize,¹⁴ and enable simple, one-step conjugation reactions. Maleimides react specifically with thiols at neutral pH, generating a stable thioether linkage (Figure 1, A).¹⁵ To participate in this reaction, the recombinant protein requires the presence of a single cysteine residue, which can be readily incorporated using site-directed mutagenesis.

Group A Streptococcus (GAS; *Streptococcus pyogenes*), which is associated with diseases including pharyngitis (sore throat) and RHD,¹⁶ was selected as a model organism for developing this platform. As over 200 strains have been identified, the development of a broadly protective vaccine requires the incorporation of multiple protective antigens,¹⁶

favoring a recombinant approach. Further, many well-defined protective GAS antigens have been reported,¹⁷⁻²⁰ providing valuable knowledge for antigen selection. For this work, peptide antigens from the GAS cell-surface M protein, which are amongst the most promising GAS vaccine targets,¹⁶ were selected. A 'string-of-beads' (polytope) approach was used (**1**, Figure 2, A) to link seven strain-specific N-terminal M protein antigens, from GAS isolates prevalent in the Australian Aboriginal population of the Northern Territory,¹⁸ to a conserved M protein conformational B cell epitope (J14i; bold sequence in J14), which is flanked by peptides designed to promote its native α -helical structure (J14: KQAEDKVK**ASREAKKQVEKALEQLEDKVK**).¹⁷ Several of these antigens, when administered as part of a synthetic LCP system, have been demonstrated to elicit long-lasting antibody mediated immunity in murine preclinical models.²¹ A universal source of T cell help (PADRE 1024.03)²² was also included to aid memory B cell production in genetically diverse populations (e.g. humans), along with a C-terminal cysteine to allow site-specific conjugation to the lipid adjuvant.

The lipid adjuvants used in this work (**2** and **3**; Figure 1, A) feature three lipoamino acids (2-aminohexadecanoic acid), a short peptide to enhance solubility under aqueous conditions, and an N-terminal maleimide for bioconjugation to **1**. As dendritic cell (DC) targeting can enhance antibody-mediated immunity, and significantly reduce the amount of antigen required to ensure effective immunity,²³ we decided to incorporate a DC targeting peptide (DCpep;²⁴ Figure 1, A) into adjuvant **2**. An additional adjuvant (**3**), incorporating a peptide without DC targeting potential (CONTROLpep;²⁴ Figure 1, A) was also produced as a control.

Herein we describe the processes used to develop and optimize our polytope GAS antigen **1** (Figure 2), synthetic lipid adjuvants (**2, 3**; Figure 1, *A*), and bioconjugation conditions, to enable the simple, high yielding production of semisynthetic lipid-adjuvanted nanoparticulate vaccines. The vaccines were produced with (**6**) or without (**7**) a DC targeting sequence, enabling the effect of this modification on antibody-levels to be assessed using a murine preclinical model. Extensive characterization of the vaccines was undertaken to confirm particle size, purity, lack of endotoxin contamination, and site-specific bioconjugation. As an indicator of the protective potential of these vaccines, antisera from subcutaneously immunized mice were evaluated for their potential to bind cell surface M proteins from a panel of GAS strains representing each antigen included in these vaccines.

Methods

Detailed methods, sequences, and characterization data are provided as supplementary information (available online at <http://www.nanomedjournal.com>).

Recombinant protein antigen

Recombinant protein antigen **1** (Figure 2, *A*; Table S1) was designed, reverse-translated, and codon optimized for expression in *Escherichia coli*. The gene (Table S2) was assembled from 18 overlapping oligonucleotides (Table S3) by PCR-based gene synthesis,²⁵ inserted into pTXB1, and mutated to generate a C-terminal cysteine fusion. The protein was expressed in BL21(DE3)-RIL (37 °C, 4 hours), with 0.5 mM isopropylthio- β -galactoside (IPTG) induction at OD₆₀₀ 0.6, and purified to homogeneity

(Figure 2, C-E) by reversed-phase high-performance liquid chromatography (RP-HPLC) after denaturing lysis and enrichment by nickel-nitrilotriacetic acid (Ni-NTA) chromatography.

Lipid adjuvant peptide synthesis

Lipid adjuvant peptides **2** and **3** (Figure 1, A) were synthesized using microwave-assisted Fmoc (9-fluorenylmethyloxycarbonyl) solid-phase peptide synthesis (SPPS). The lipid adjuvant was incorporated using a Dde (1-(4,4-dimethyl-2,6-dioxocyclohexylidene)ethyl)-protected 2-aminohexadecanoic acid lipoamino acid.²⁶ 6-Maleimidohexanoic acid was synthesized as previously described,¹⁴ with modifications (see supplemental information). The lipoamino acid and 6-maleimidohexanoic acid were incorporated without microwave heating. Peptides were cleaved from the resin using trifluoroacetic acid (TFA), and purified to homogeneity by RP-HPLC on a C4 stationary phase (Figure S1, B and C).

Bioconjugation reaction

Bioconjugation reactions (Figure 1, A) were performed at 37 °C for 30 min in 6 M guanidine-HCl, 50 mM sodium phosphate pH 7.3, 20 % acetonitrile, 5 mM ethylenediaminetetraacetic acid (EDTA) containing ~ 2 mg/mL of **1** and 4-5 eq of **2** or **3**. Adjuvants (**2**, **3**) were dissolved in dimethyl sulfoxide (DMSO; to 4 % (v/v) final concentration) before their addition. Lipoprotein products (**4**, **5**) were purified by RP-HPLC on a C4 stationary phase (Figure S2).

His-tag removal

Lipoproteins (**4**, **5**) were dissolved to 1 mg/mL in phosphate buffered saline (PBS). Thrombin from human plasma (6 U/mg of **4** or **5**) was added, and the mixture incubated at 37 °C for 3 h. Lipoprotein products (**6**, **7**) were purified by RP-HPLC on a C4 stationary phase.

Characterization of lipoprotein vaccines

Lipoprotein vaccines were characterized according to the following parameters: A. molecular weight (electrospray ionization mass spectrometry (ESI-MS), and sodium dodecyl sulfate polyacrylamide gel electrophoresis (SDS-PAGE); Figure 1, *C* and *D*; Figure S3; Figure S4), B. purity (RP-HPLC, SDS-PAGE, ESI-MS; Figure 1, *C* and *D*; Figure S3, Figure S4), C. correct sequence (Sanger sequencing, ESI-MS, peptide mass fingerprinting (PMF) after Asp-N digestion of **4**; Figure 1, *C* and *D*; Figure S5, *C*), D. site-specific conjugation (PMF; Figure S5), E. particle size (dynamic light scattering (DLS), transmission electron microscopy (TEM); Figure 3, *A* and *B*), F. endotoxin contamination (calorimetric *Limulus* ameobocyte lysate (LAL) assay), G. oligonucleotide contamination (agarose electrophoresis with ethidium bromide staining).

Immunization

Immunization was performed under protocols approved by the Griffith University (BDD/06/10/AEC) and University of Queensland (SCMB/GRIFITH/005/12/MERCK/NIH/NHF/NHMRC) animal ethics committees. The

immunization schedule was based on kinetic data for antibody induction obtained from mice immunized with a synthetic LCP system (incorporating three GAS M protein antigens).²⁷ Each immunogen (**1**, **6**, and **7**; 30 µg/injection in 50 µL; A₂₈₀ quantified stock solutions) was administered subcutaneously at the tail base in C57BL/6J (H-2^b) mice (5/group). PBS sham immunization was used as a negative control. Mice receiving **1** were primed with a 1:1 emulsion of PBS (containing **1**) and complete Freund's adjuvant (CFA). Administration of lipoproteins (**6**, **7**), and boosting with **1**, was performed with PBS solubilized immunogens. Mice were boosted 21 days after priming, and received a further 2 boosts at 7-day intervals. Final bleeds were collected from the tail artery one week after the final boost.

Enzyme-linked immunosorbent assay (ELISA)

An ELISA was performed to measure antigen-specific serum IgG antibody titers against the eight M protein antigens, for each individual mouse, essentially as described.¹⁷ Antibody titers were defined as the lowest dilution with an OD₄₅₀ value greater than three standard deviations above the mean absorbance of control wells (sera from PBS immunized mice). ELISA data (Figure 4) is expressed as mean antigen-specific IgG antibody titer. Error bars indicate the standard error of the mean (SEM). Raw data is provided as supplemental information (Figure S6).

Confocal microscopy

Confocal immunofluorescence microscopy was used to qualitatively demonstrate the binding of pooled antibodies elicited in response to vaccination with **1** (primed with

CFA), or **6** to the surface of GAS strains represented in our vaccine (Figure 5, *B*), as described.²⁸ The following strains were used: 88/30 (*emm97*), PL1 (*emm54*), NS1 (*emm100*), Y504S (*emm11*), BSA10 (*emm2.3*), NS27 (*emm91*), NS5 (*emm101*), and pM1 (*emm1*; for J14). The confocal microscope was calibrated for positive and negative samples using pM1 GAS and murine antisera against recombinant M1 M protein or arginine deiminase (ADI)¹⁹ as positive controls, or antisera from sham (PBS) immunized mice as a negative control (Figure 5, *A*).

Results

Production of semisynthetic lipoprotein vaccine building blocks

Recombinant protein **1** expressed as insoluble inclusion bodies and in the soluble cytoplasmic fraction (Figure 2, *B*). Purification yielded at least 20 mg of homogeneous protein (per liter culture), suitable for conjugation to lipid adjuvants **2** or **3**. The lipid adjuvants were readily synthesized by Fmoc-SPPS and purified to homogeneity (Figure S1, *B* and *C*) with a moderate overall yield (**2**: 43 %; **3**: 38 %). Attempts to simplify the lipid adjuvant peptides, through deletion of the peptide (DCpep or CONTROLpep) sequences, yielded hydrophobic molecules that were challenging to purify or use for the bioconjugation reactions.

Maleimide conjugation reaction

The conditions used for bioconjugation of recombinant protein **1** to the lipid adjuvants (**2**, **3**; Figure 1, *A*) were optimized. High yielding (**4**: 71 %; **5**: 89 %), rapid (< 15 min),

and complete reactions were achieved at 37 °C under denaturing conditions (6 M guanidine), with 20 % (v/v) acetonitrile as a cosolvent. Lipid adjuvants (**2** or **3**; 4-5-fold excess over **1**) were added to the reaction after dissolving in DMSO. The direct addition of **2** or **3**, or use of *N,N*-dimethylformamide (DMF) for their dissolution resulted in lower product yields (e.g. 26 % yield for **5** when **3** was dissolved in DMF). Further, the addition of tris(2-carboxyethyl)phosphine (TCEP) to maintain a reduced cysteine, generated an addition product with **2** or **3**, that was unable to participate in the bioconjugation reaction. Lipid adjuvant attachment was also found to progress under native conditions (e.g. in PBS), with slower reaction kinetics, some precipitation of **2** or **3**, and reduced reaction progress. Lipoprotein products (**4**, **5**; Figure 1, *A*) were easily removed from other reaction components by RP-HPLC (Figure 1, *B*), enabling their simple purification. The His-tags were subsequently removed using thrombin (Figure 1, *A*), in a high yielding (**6**: 89 %; **7**: 75 %) and clean reaction (Figure 1, *C* and *D*).

Characterization of lipoprotein vaccines

The molecular weights of lipoprotein products **6** and **7** were confirmed by ESI-MS (Figure 1, *C* and *D*), with each product obtained at greater than 99 % purity (by analytical RP-HPLC area under the curve analysis). Evidence for site-specific lipid adjuvant conjugation was obtained via Asp-N digestion of **4**, followed by PMF using RP-HPLC and ESI-MS. This experiment generated a single hydrophobic peptide, corresponding with the C-terminus (25 amino acids) of **1** conjugated to **2** (Figure S5, *B*), with the other proteolytic peptides providing 79.8 % coverage of the lipoprotein **4** sequence (Figure S5, *C*). The particle size of the purified vaccines (in PBS) was analyzed by TEM (Figure 3, *A*) and DLS (Figure 3, *B*), revealing single mono- (**6** polydispersity: 15

%) or medium-disperse (**7** polydispersity: 24 %) nanoparticle populations, with a 40 nm average particle size (**6**: 39 nm; **7**: 43 nm). The vaccines were further analyzed for the presence of immunostimulatory contaminants using an LAL endotoxin assay, and agarose gel electrophoresis. Endotoxin levels were below the standard curve lower limit (< 0.1 EU/mL), indicating that endotoxin contamination was significantly below pharmacopoeial limits (USP/BP), and no oligonucleotide contamination was detected (data not shown).

Assessment of the immune response to lipoproteins

Systemic antigen-specific IgG antibody titers were quantified by ELISA at the final bleed (day 42) (Figure 4; Figure S6). Antibodies targeting all eight M protein antigens were detected in mice immunized with lipoproteins **6** or **7**, in addition to the positive control group (mice primed with **1** in CFA) (Figure 4; Figure S6), verifying that the lipoprotein vaccines possess inbuilt adjuvant activity. A comparison of the antigen-specific antibody levels in mice administered **6** or **7** revealed a trend towards higher antibody levels in mice immunized with **6** (Figure 4; Figure S6), which contains a DC targeting peptide (DCpep). This relationship was statistically significant for the BSA10 ($P \leq 0.01$) and NS27 ($P \leq 0.05$) antigens.

The level of anti-Y504S antibodies was observed to be 1-5 orders of magnitude lower than observed for other antigens (Figure 4; Figure S6). This effect was apparent for both the lipoprotein (**6**, **7**) and positive control (**1** with CFA priming) groups. Anti-J14 antibodies were also considerably lower (~ 1400-fold) in the lipoprotein groups (4.6×10^2 mean titer for **6**) compared with the positive control group (6.3×10^5 mean titer; P

≤ 0.05) (Figure 4; Figure S6). The level of these antibodies in the positive control group was similar to the levels observed for antigens other than Y504S, with high levels of anti-p145 antibodies (2.9×10^5 mean titer), which measure anti-J14 antibody binding to the correctly folded J14i antigen,¹⁷ also detected.

Confocal immunofluorescence microscopy was used to qualitatively assess the binding of antibodies to a panel of GAS strains representing the eight vaccine M protein antigens (Figure 5, B). Similar to the ELISA data, strong binding was observed in all strains, where antisera from the positive control group were used, with the exception of Y504S. Similar, but visually weaker binding was observed where sera from lipoprotein 6 immunized mice were assessed, with reduced binding to pM1 GAS (which only includes the J14i antigen in its M protein) in addition to the Y504S strain.

Discussion

The technology established herein allows for simple and efficient generation of lipid-adjuvanted protein vaccines. It is ideal for vaccines incorporating denatured protein antigens, for which fast and complete bioconjugation reactions were observed. This favors the polytope approach, since the majority of epitopes used (N-terminal M protein antigens and PADRE1024.03) do not require a specific fold,²⁹ and J14 readily refolds on its own.^{17, 30} In addition to this advantage, polytopes enable the incorporation of multiple defined epitopes within a single immunogen, greatly enhancing the capacity to elicit broad protective immunity compared with single epitope approaches,³¹ and permit the incorporation of large antigens that are beyond the size accessible to peptide synthesis.^{11, 31} The technology may also be used with full-length natural proteins, their mutants, or immunogenic fragments. This requires the addition of a C-terminal or

internal cysteine residue to enable maleimide conjugation, with N-terminal fusions discouraged due to their reactivity with aldehyde/ketone metabolites during expression.³² Proteins that contain cysteine may also be incorporated where conservative cysteine mutations (e.g. to serine or alanine) maintain the capacity to elicit protective immunity. Alternatively, where cysteine residues are buried, or involved in disulfide bonds, this approach may prove successful if native, non-reducing conjugation conditions are used.

Synthesis of polytope genes is efficient, relatively inexpensive, and provides access to improved expression yields through codon optimization for industrial scale expression hosts.³³ The gene used herein could be readily assembled by gene synthesis PCR²⁵ (or alternatively outsourced e.g. to DNA2.0), and inserted into expression vectors using restriction-free cloning.³⁴ The gene product could then be overexpressed in *E. coli*, and purified under denaturing-reducing conditions to solubilize inclusion bodies and maintain cysteine residues in a reduced state. In addition to the aforementioned advantages, the purification of polytope antigens under denaturing conditions is of significant advantage where protein is predominantly expressed in inclusion bodies, as protein enrichment can be achieved through simple lysis, centrifugation, and detergent washes, and purification achieved without the need for costly affinity purification steps (e.g. by size exclusion, or ammonium sulfate cuts).³⁵

Several approaches were taken to optimize the bioconjugation reaction conditions. These included: avoiding thiol (e.g. 2-ME) or phosphine (e.g. TCEP) reducing agents, which were detrimental to the conjugation reaction; the addition of EDTA to prevent metal catalyzed cysteine oxidation;¹⁵ maintaining near neutral pH to reduce the

oxidation rate; and the addition of lipid adjuvants in excess, to drive reactions to completion. The hydrophobic nature of the lipid adjuvants necessitated solubilization in an organic solvent prior to use, with DMSO proving ideal (fast reaction rates (<15 min) and high yields (> 71 %)), despite concerns about its capacity to promote cysteine oxidation.³⁶

Prior to assessing lipoprotein vaccines in mice, the His-tags were removed (Figure 1, A) in order to minimize effects on J14 folding, or reduction in vaccine efficacy due to tag-directed immunity.³⁷ Quantified vaccine stock solutions were then produced to ensure administration of equivalent vaccine doses, and further characterized to verify their freedom from endotoxin contamination. This step is important for immunogens expressed in *E. coli*, which produces endotoxins that could contaminate the final product.³⁸ Such contamination could contribute to adjuvant activity, complicating the assessment of lipoprotein vaccine associated immunostimulation.

The site-specific nature of the bioconjugation reaction is also important for the success of this platform because it ensures that a single vaccine product is produced, which can be characterized at the molecular level. Since the maleimide-species was used in excess, we sought evidence that adjuvant conjugation occurred exclusively through the cysteine. This was important, as maleimides may also react with amines, although at a slower rate under the pH conditions used.¹⁵ A PMF approach provided an ideal means to assess the site-specificity of the conjugation reaction. By selecting a protease that does not cut within the lipid adjuvant, proteolytic peptides fused to the lipid adjuvant are specifically generated at sites where conjugation occurred. The extreme hydrophobicity of these peptides enables their sorting from other proteolytic species by

RP-HPLC for subsequent characterization by ESI-MS. In this case Asp-N digestion of **4** generated a single hydrophobic peptide, corresponding with conjugation through the C-terminus of **1** (Figure S5, *A* and *B*). This data strongly supported that conjugation was site-specific and occurred through the C-terminal cysteine.

The lipoprotein vaccines were further characterized by TEM and DLS to investigate their capacity to form particles following addition to aqueous buffers. Both techniques revealed that lipoproteins **6** and **7** form ~ 40 nm diameter nanoparticles (Figure 3, *A* and *B*). This information was important because particle size is known to have a significant effect on antigen transport to secondary lymphoid organs, uptake by antigen presenting cells, cross-presentation, and potency of the immune response.³⁹ Particles in the 10-200 nm range (with ~ 40 nm particles considered optimal)³⁹ enter lymph vessels through gaps between endothelial cells. Following parenteral administration, these particles reach the lymph node within hours, and can access both B and T cell regions. In comparison, particles that are larger than 200-500 nm require cellular transport (e.g. by DCs) to reach the lymphatic system.³⁹ This takes upwards of 24 hours, reducing the amount of native antigen presented to B cells, and restricting access to T cell regions in the lymph nodes. Based on this knowledge, our nanoparticles appear to fall within the optimum size range for eliciting potent antibody-mediated immunity, which is desirable for this application.

Lipoprotein vaccines (**6**, **7**) were administered subcutaneously to C57BL/6J mice to assess their ability to stimulate protective antibody-mediated immunity, without the need for coadministration with an adjuvant. Polytope **1**, with CFA priming, was administered as a positive control. This combination is not suitable for human use as

CFA is associated with significant toxicity.⁴⁰ Both polytope (**1** primed with CFA) and lipoprotein (**6**, **7**) vaccines raised systemic IgG antibodies against all eight polytope antigens (Figure 4; Figure S6). This validated that the polytope approach was suitable for the selected antigens, and verified the immunostimulatory activity of the lipid adjuvants, respectively. A trend towards higher systemic antigen-specific IgG antibody titers was also observed in mice immunized with **6** compared with **7** (Figure 4; Figure S6). This is likely because lipoprotein **6** incorporates DCpep, which has been demonstrated to specifically bind to the surface of DCs from various animal species.²⁴ Antigen fusions with DCpep provide a means to target DCs, and have been observed to increase antigen uptake, processing and presentation, leading to more potent antigen-specific immunity.^{24, 41, 42} Although antigen-specific IgG antibodies were elicited against each polytope antigen, Y504S₁₋₂₀ was weakly immunogenic in the context of the polytope (Figure 4; Figure S6). Similar observations were made for J14 in the lipoprotein groups, while high levels of anti-J14 and p145 antibodies were observed for CFA primed mice (Figure 4; Figure S6).

To further characterize the functional significance of antibodies raised against our lipoprotein vaccines, we turned to a confocal immunofluorescence microscopy approach. Antibodies targeting N-terminal M protein antigens¹⁸ and J14⁴³ have been demonstrated to elicit protective (i.e. opsonic) antibody responses. By investigating the binding of antibodies elicited against our lipoproteins to the eight vaccine represented GAS strains, the protective potential offered by these antibodies can be assessed. This assay also evaluates binding in the context of the native bacterium, ensuring native M protein folding, and maintains factors that may reduce the antibody binding capacity (e.g. the hyaluronic acid capsule).²⁸ The results of this assay (Figure 5, *B*) demonstrated

that antibodies raised against lipoprotein 6 bound all eight GAS strains represented in the vaccine, although fluorescence associated with pM1 (which expresses the J14i epitope) or Y504S (*emm11*) binding was lower than for the other antigens.

Overall, this research has provided a method to enable the simple, high yielding conjugation of recombinant protein antigens to LCP-based lipid adjuvants. The capacity to combine recombinant and synthetic approaches enables the production of vaccines of a size greater than would be accessible by synthetic means alone, with the site-specific bioconjugation chemistry generating a chemically defined product. The polytope approach offers further advantages by permitting the incorporation of many defined peptide epitopes, producing a more focused immune response compared with the use of whole proteins, and enables the incorporation of epitopes from multiple sources. As a model for developing this platform, the lipid adjuvant was conjugated to a polytope incorporating eight GAS M protein antigens. This construct displayed self-adjuvanting activity, formed particles of an optimal size for generating antibody-mediated immunity, and elicited antibodies against each polytope antigen that bound their respective GAS strain.

Acknowledgements

We would like to acknowledge Professor Kirill Alexandrov, Saranya Chandrudu, Thalia Guerin, Regina Hartmann, Dr. Benjamin Schulz, and Dr. Mehruz Zaman for their assistance. The authors acknowledge the facilities, and the scientific and technical assistance, of the Australian Microscopy & Microanalysis Research Facility at the Centre for Microscopy and Microanalysis, The University of Queensland.

References

1. Pulendran B, Ahmed R. Immunological mechanisms of vaccination. *Nat Immunol* 2011;**12**:509-17.
2. Nossal GJ. Vaccines of the future. *Vaccine* 2011;**29**:D111-D5.
3. Hedayat M, Takeda K, Rezaei N. Prophylactic and therapeutic implications of toll-like receptor ligands. *Med Res Rev* 2012;**32**:294-325.
4. Gibbons WA, Hughes RA, Charalambous M, Christodoulou M, Szeto A, Aulabaugh AE, et al. Lipidic peptides .1. Synthesis, resolution and structural elucidation of lipidic amino-acids and their homo-oligomers and heterooligomers. *Liebigs Ann Chem* 1990;1175-83.
5. Moyle PM, Toth I. Self-adjuvanting lipopeptide vaccines. *Curr Med Chem* 2008;**15**:506-16.
6. Zaman M, Abdel-Aal AB, Fujita Y, Ziora ZM, Batzloff MR, Good MF, et al. Structure-activity relationship for the development of a self-adjuvanting mucosally active lipopeptide vaccine against *Streptococcus pyogenes*. *J Med Chem* 2012;**55**:8515-23.
7. Moyle PM, Olive C, Ho MF, Pandey M, Dyer J, Suhrbier A, et al. Toward the development of prophylactic and therapeutic human papillomavirus type-16 lipopeptide vaccines. *J Med Chem* 2007;**50**:4721-7.
8. Zaman M, Abdel-Aal AB, Fujita Y, Phillipps KS, Batzloff MR, Good MF, et al. Immunological evaluation of lipopeptide group A streptococcus (GAS) vaccine: structure-activity relationship. *PLoS one* 2012;**7**:e30146.
9. Phillipps KS, Wykes MN, Liu XQ, Brown M, Blanchfield J, Toth I. A novel synthetic adjuvant enhances dendritic cell function. *Immunology* 2009;**128**:e582-e8.

10. Moisa AA, Kolesanova EF. Synthetic peptide vaccines. *Biochemistry (Moscow) Supplement Series B: Biomedical Chemistry* 2011;**4**:321-32.
11. Kent SB. Total chemical synthesis of proteins. *Chem Soc Rev* 2009;**38**:338-51.
12. Cox MM. Recombinant protein vaccines produced in insect cells. *Vaccine* 2012;**30**:1759-66.
13. Zom GG, Khan S, Filippov DV, Ossendorp F. TLR ligand-peptide conjugate vaccines: toward clinical application. *Adv Immunol* 2012;**114**:177-201.
14. de Figueiredo RM, Oczipka P, Frohlich R, Christmann M. Synthesis of 4-maleimidobutyric acid and related maleimides. *Synthesis* 2008;1316-8.
15. Hermanson GT. The chemistry of reactive groups. In: *Bioconjugate Techniques*. 2nd ed. Academic Press: Amsterdam; 2008, p. 169-212.
16. Cole JN, Barnett TC, Nizet V, Walker MJ. Molecular insight into invasive group A streptococcal disease. *Nat Rev Microbiol* 2011;**9**:724-36.
17. Hayman WA, Brandt ER, Relf WA, Cooper J, Saul A, Good MF. Mapping the minimal murine T cell and B cell epitopes within a peptide vaccine candidate from the conserved region of the M protein of group A streptococcus. *Int Immunol* 1997;**9**:1723-33.
18. Brandt ER, Teh T, Relf WA, Hobb RI, Good MF. Protective and nonprotective epitopes from amino termini of M proteins from Australian aboriginal isolates and reference strains of group A streptococci. *Infect Immun* 2000;**68**:6587-94.
19. Henningham A, Chiarot E, Gillen CM, Cole JN, Rohde M, Fulde M, et al. Conserved anchorless surface proteins as group A streptococcal vaccine candidates. *J Mol Med* 2012;**90**:1197-207.

20. Bensi G, Mora M, Tuscano G, Biagini M, Chiarot E, Bombaci M, et al. Multi high-throughput approach for highly selective identification of vaccine candidates: the Group A Streptococcus case. *Mol Cell Proteomics* 2012;**11**:M111.015693.
21. Olive C, Ho MF, Dyer J, Lincoln D, Barozzi N, Toth I, et al. Immunization with a tetraepitopic lipid core peptide vaccine construct induces broadly protective immune responses against group A streptococcus. *The Journal of infectious diseases* 2006;**193**:1666-76.
22. Alexander J, Sidney J, Southwood S, Ruppert J, Oseroff C, Maewal A, et al. Development of high potency universal DR-restricted helper epitopes by modification of high affinity DR-blocking peptides. *Immunity* 1994;**1**:751-61.
23. Caminschi I, Shortman K. Boosting antibody responses by targeting antigens to dendritic cells. *Trends Immunol* 2012;**33**:71-7.
24. Curiel TJ, Morris C, Brumlik M, Landry SJ, Finstad K, Nelson A, et al. Peptides identified through phage display direct immunogenic antigen to dendritic cells. *J Immunol* 2004;**172**:7425-31.
25. Wu G, Wolf JB, Ibrahim AF, Vadasz S, Gunasinghe M, Freeland SJ. Simplified gene synthesis: A one-step approach to PCR-based gene construction. *J Biotechnol* 2006;**124**:496-503.
26. Ross BP, Falconer RA, Toth I. N-1-(4,4-dimethyl-2,6-dioxocyclohex-1-ylidene)ethyl (N-Dde) lipoamino acids. *Molbank* 2008;**2**:M566.
27. Moyle PM, Olive C, Ho MF, Good MF, Toth I. Synthesis of a highly pure lipid core peptide based self-adjuvanting triepitopic group A streptococcal vaccine, and subsequent immunological evaluation. *J Med Chem* 2006;**49**:6364-70.
28. Bauer MJ, Georgousakis MM, Vu T, Henningham A, Hofmann A, Rettel M, et al. Evaluation of novel *Streptococcus pyogenes* vaccine candidates incorporating

- multiple conserved sequences from the C-repeat region of the M-protein. *Vaccine* 2012;**30**:2197-205.
29. Fischetti VA. Streptococcal M protein: molecular design and biological behavior. *Clin Microbiol Rev* 1989;**2**:285-314.
 30. Georgousakis MM, Hofmann A, Batzloff MR, McMillan DJ, Sriprakash KS. Structural optimisation of a conformational epitope improves antigenicity when expressed as a recombinant fusion protein. *Vaccine* 2009;**27**:6799-806.
 31. Babiuk LA. Broadening the approaches to developing more effective vaccines. *Vaccine* 1999;**17**:1587-95.
 32. Gentle IE, De Souza DP, Baca M. Direct production of proteins with N-terminal cysteine for site-specific conjugation. *Bioconjug Chem* 2004;**15**:658-63.
 33. Hughes RA, Miklos AE, Ellington AD. Gene synthesis: methods and applications. *Methods Enzymol* 2011;**498**:277-309.
 34. Bryksin AV, Matsumura I. Overlap extension PCR cloning: a simple and reliable way to create recombinant plasmids. *BioTechniques* 2010;**48**:463-5.
 35. Jungbauer A, Kaar W. Current status of technical protein refolding. *J Biotechnol* 2007;**128**:587-96.
 36. Tam JP, Wu CR, Liu W, Zhang JW. Disulfide bond formation in peptides by dimethyl sulfoxide. Scope and applications. *J Am Chem Soc* 1991;**113**:6657-62.
 37. Khan F, Legler PM, Mease RM, Duncan EH, Bergmann-Leitner ES, Angov E. Histidine affinity tags affect MSP₁₄₂ structural stability and immunodominance in mice. *Biotechnol J* 2012;**7**:133-47.
 38. Magalhaes PO, Lopes AM, Mazzola PG, Rangel-Yagui C, Penna TC, Pessoa A, Jr. Methods of endotoxin removal from biological preparations: a review. *J Pharm Pharm Sci* 2007;**10**:388-404.

39. Bachmann MF, Jennings GT. Vaccine delivery: a matter of size, geometry, kinetics and molecular patterns. *Nat Rev Immunol* 2010;**10**:787-96.
40. Chapel HM, August PJ. Report of nine cases of accidental injury to man with Freund's complete adjuvant. *Clin Exp Immunol* 1976;**24**:538-41.
41. Mohamadzadeh M, Durmaz E, Zadeh M, Pakanati KC, Gramarossa M, Cohran V, et al. Targeted expression of anthrax protective antigen by *Lactobacillus gasseri* as an anthrax vaccine. *Future microbiology* 2010;**5**:1289-96.
42. Erskine CL, Krco CJ, Hedin KE, Borson ND, Kalli KR, Behrens MD, et al. MHC class II epitope nesting modulates dendritic cell function and improves generation of antigen-specific CD4 helper T cells. *J Immunol* 2011;**187**:316-24.
43. Vohra H, Dey N, Gupta S, Sharma AK, Kumar R, McMillan D, et al. M protein conserved region antibodies opsonise multiple strains of *Streptococcus pyogenes* with sequence variations in C-repeats. *Res Microbiol* 2005;**156**:575-82.

Figure Legends

Figure 1. Maleimide conjugation reaction. **(A)** The conjugation between recombinant antigen **1** and lipid adjuvant peptides **2** or **3** and subsequent His-tag cleavage is depicted, along with the structure of the lipid adjuvant peptides. **(B)** HPLC chromatogram for the conjugation of **1** and **2**, demonstrating the separation between starting material (**1**, **2**) and product (**4**). **(C)** and **(D)** HPLC, reconstructed mass spectra, and SDS-PAGE data for purified lipoproteins **6** and **7**, respectively.

Figure 2. Synthesis, cloning and expression of recombinant polytope antigen **1**. **(A)** Scheme depicting the production of recombinant polytope **1**, with the antigen arrangement and protein sequence shown. **(B)** Analysis of protein **1** expression by SDS-PAGE. Lanes show uninduced (UN) and induced (IN) whole cell fractions, as well as inclusion body (IB) and soluble cytoplasmic fractions following lysis. **(C)** Reconstructed mass spectra, **(D)** HPLC, and **(E)** SDS-PAGE data for purified antigen **1**.

Figure 3. Lipoproteins **6** and **7** form nanoparticles in aqueous buffers. **(A)** TEM demonstrates the formation of lipoprotein nanoparticles. **(B)** Dynamic light scattering (6 replicates) shows that these particles have an average diameter of ~ 40 nm.

Figure 4. Assessment of antigen-mediated immunity elicited in response to subcutaneous immunization with recombinant antigen **1** (primed with CFA), lipoprotein **6** (includes DCpep) or **7** (includes CONTROLpep), or PBS sham (negative control). An ELISA was used to measure the antigen-specific serum IgG antibody titers (\log_{10}), against the eight polytope antigens, from individual sera collected one-week

after the final boost. Plates were coated with synthetic peptide antigens. The capacity for antibodies against J14 to bind the folded J14i conformational epitope was demonstrated using p145. Data is expressed as mean antigen-specific IgG antibody titer. Error bars represent the standard error of the mean (SEM).

Figure 5. Confocal immunofluorescence (right panels) and DIC (left panels) microscopy of GAS strains represented within the polytope sequence (pM1 M protein incorporates J14i). **(A)** Positive and negative controls. Antisera from mice immunized with M1 or ADI (with CFA priming) were used as positive controls, with pooled antisera from PBS sham immunized mice used as a negative control for binding pM1 GAS. **(B)** Stationary phase bacteria were incubated with pooled antisera (1:200) from mice immunized with **1** (primed with CFA), lipoprotein **6**, or PBS sham (negative control), labeled with goat anti-mouse IgG-FITC, and viewed with a 100× oil-immersion objective. An asterisk (*; upper right) indicates that a 1:50 dilution of primary antisera was used. Scale bars (upper left) indicate 2 μm.

Figure 1

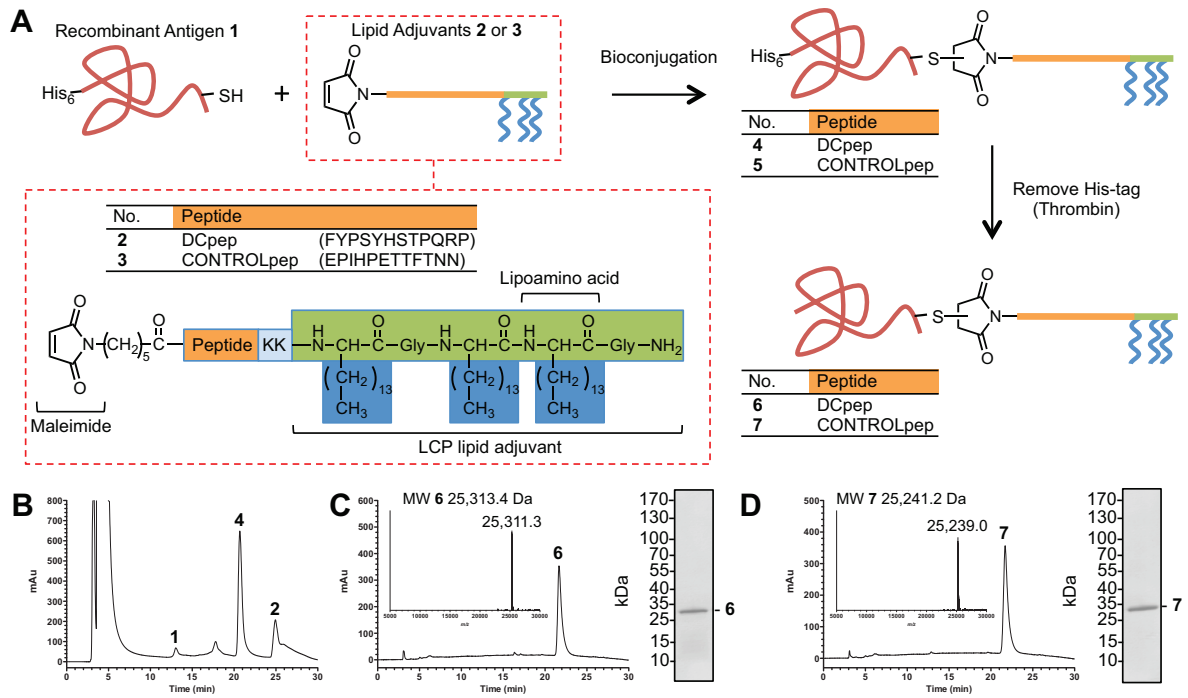


Figure 2

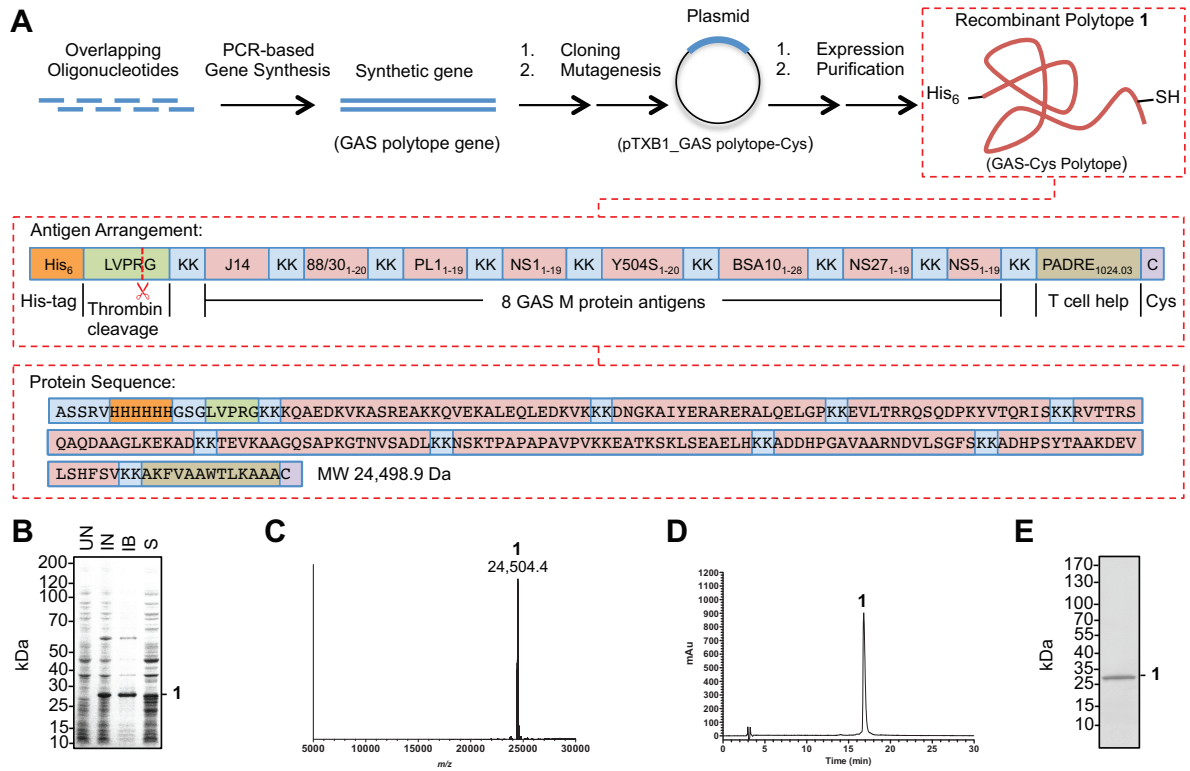


Figure 3

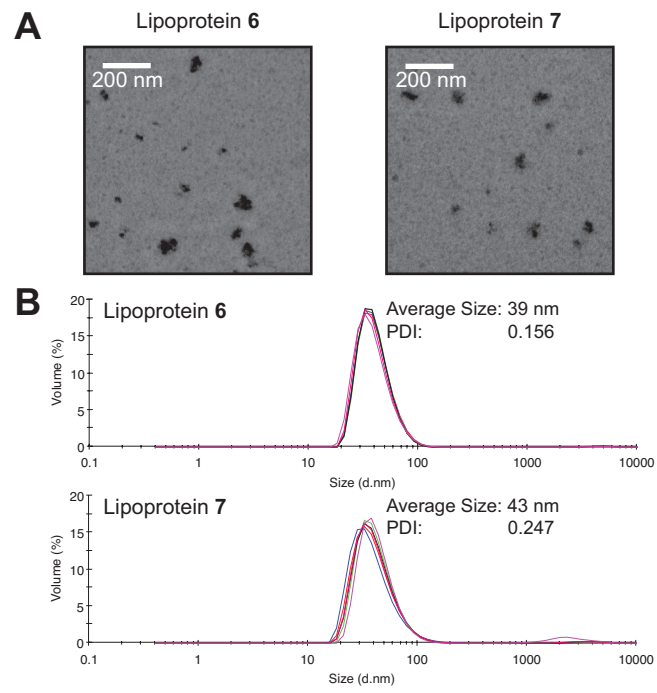


Figure 4

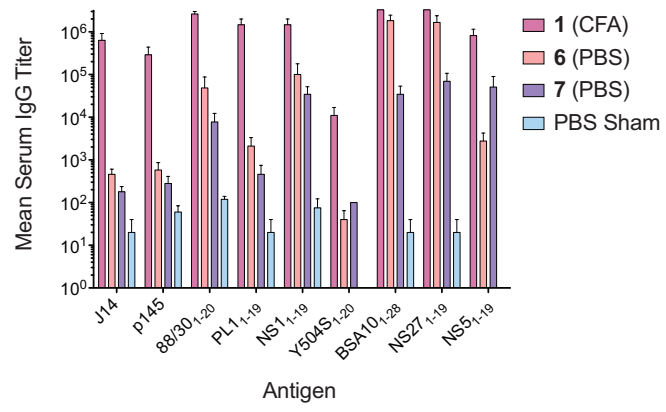
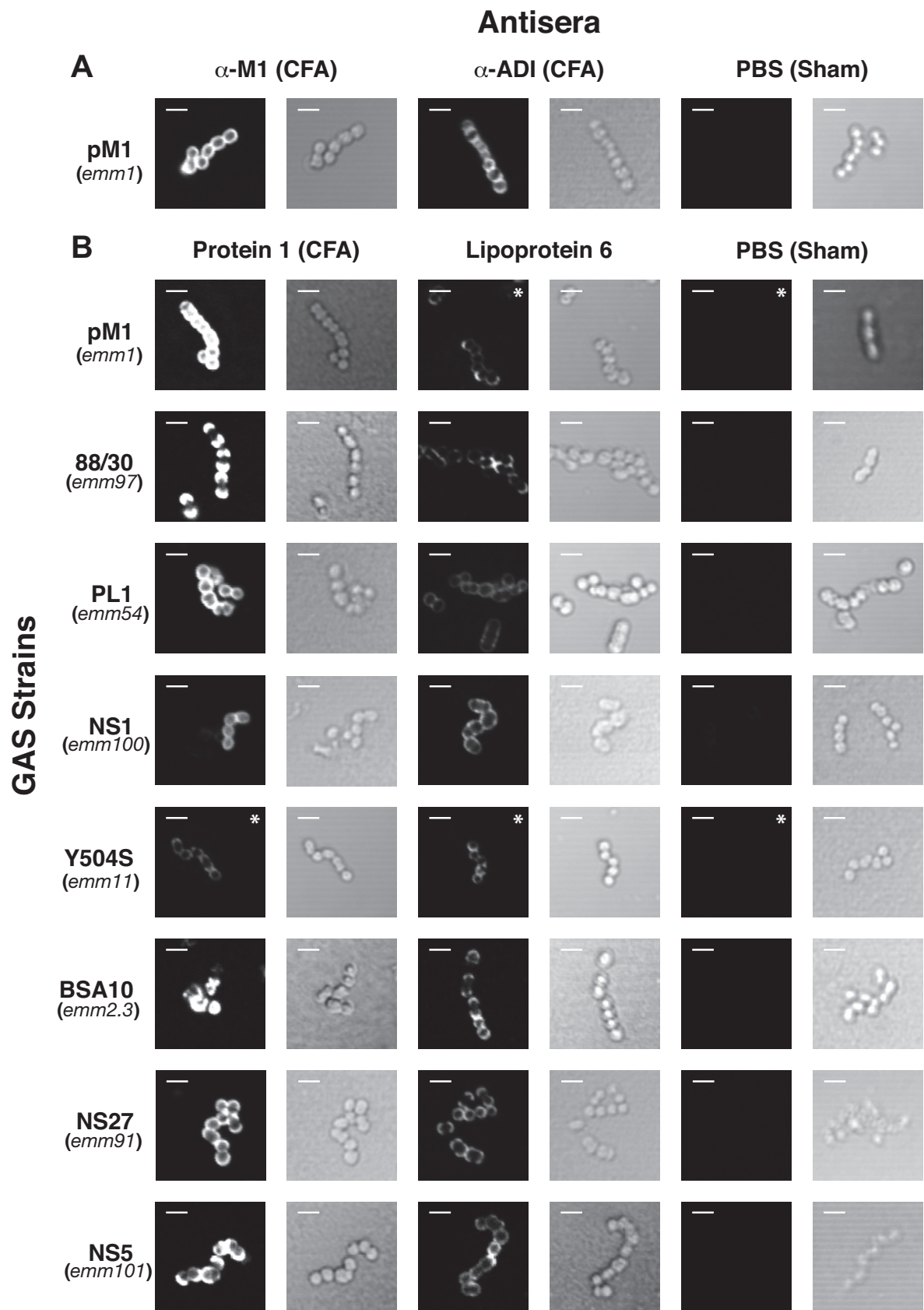


Figure 5



An Efficient, Chemically-Defined Semisynthetic Lipid-Adjuvanted Nanoparticulate Vaccine Development System

Peter M. Moyle^{a,b}, Jon Hartas^c, Anna Henningham^a, Michael R. Batzloff^c, Michael F. Good^c, Istvan Toth^{a,b,d}

^a School of Chemistry and Molecular Biosciences, The University of Queensland, St Lucia 4072, QLD, AUSTRALIA

^b Institute for Molecular Biosciences, The University of Queensland, St Lucia 4072, QLD, AUSTRALIA

^c Institute for Glycomics, Griffith University, Southport 4222, QLD, AUSTRALIA

^d School of Pharmacy, The University of Queensland, Woolloongabba 4102, QLD, AUSTRALIA

Table of Contents

Statement of author contributions	S2
Materials	S2
Equipment	S2
6-Maleimidohexanoic acid synthesis	S3
2-Acetyldimedone (Dde-OH) synthesis	S4
Dde-C16-OH synthesis	S4
Peptide synthesis	S5
Peptide analytical data	S6
PCR-based gene synthesis	S6
Restriction-free cloning	S6
Site-directed mutagenesis	S7
Expression of polytope 1	S7
Conjugation of polytope 1 and lipid adjuvants 2 or 3	S7
Thrombin cleavage of hexahistidine-tags	S7
Protein analytical data	S8
Peptide mass fingerprinting	S8
Stock solutions for immunization	S9
Endotoxin testing	S9
Immunization and blood collection	S10
Statistics	S10
Confocal Microscopy	S10
Table S1. Protein/peptide sequences	S12
Table S2. DNA sequences	S13
Table S3. PCR-based gene synthesis oligonucleotides	S14
Figure S1. Analytical data for 1-3	S15
Figure S2	S16
Figure S3	S17
Figure S4	S18
Figure S5	S19
Figure S6	S20
References	S21

Statement of Author Contributions. P.M.M wrote the manuscript, envisioned project, designed and conducted experiments (synthesis, cloning, protein expression, characterization, immunization, ELISA, microscopy, and data analysis). J.H. and M.F.B designed and conducted experiments (immunization and ELISA). A.H. conducted experiments (microscopy). I.T. provided leadership, funding, equipment, and assisted in manuscript preparation. M.F.G. provided equipment, reagents and support.

General:

Materials and Methods

Materials. Fmoc (fluorenylmethoxycarbonyl)-L-amino acids, *O*-(7-Azabenzotriazol-1-yl)-*N,N,N',N'*-tetramethyluronium hexafluorophosphate (HATU), 2-(1H-benzotriazol-1-yl)-1,1,3,3-tetramethyluronium hexafluorophosphate (HBTU) were purchased from Mimotopes (Clayton, VIC, Australia). Rink amide MBHA resin (100-200 mesh; 0.59 mmol/g), methylene chloride (DCM; ACS grade), methanol (HPLC grade), *N,N*-dimethylformamide (DMF; peptide synthesis grade), and trifluoroacetic acid (TFA) were purchased from Merck Millipore (Kilsyth, VIC, Australia). MeCN (HPLC grade), and maleic anhydride were from Scharlau (Barcelona, Spain). Deuterated NMR solvents were purchased from Cambridge Isotope Laboratories, (Andover, MA, USA). Lysogeny Broth (LB; Miller's formulation), and IPTG were from Amresco (Solon, OH, USA). Thrombin from human plasma (≥ 1000 NIH units/mg protein; 0.5 U/ μ L in PBS; T7009), endoproteinase Asp-N (from *Pseudomonas fragi* mutant strain; 40 μ g/mL in 10 mM Tris-Cl pH 8; P3303), and complete Freund's adjuvant were from Sigma-Aldrich. The pTXB1 vector was from New England Biolabs (NEB; Ipswich, MA, USA). Phusion high-fidelity DNA polymerase, HisPur Nickel-nitriloacetic acid (Ni-NTA) resin, and dNTPs were from Thermo Scientific (Scoresby, VIC, Australia). The QuikChange XL II site-directed mutagenesis kit and BL21-codonplus (DE3)-RIL were from Agilent (La Jolla, CA, USA). Goat α -mouse IgG (H+L)-HRP conjugate was from Bio-Rad Laboratories (Gladesville, NSW, Australia). KOD DNA polymerase, and human plasma IgG (Calbiochem) was from Merck Millipore (Kilsyth, VIC, Australia). DNA purification kits (QIAprep spin minikit, QIAquick gel extraction kit, and QIAquick PCR purification kit) were from Qiagen (Chadstone, VIC, Australia). Oligonucleotides were purchased from Integrated DNA Technologies (IDT) (Coralville, IA, USA) with standard desalting. Peptide antigens for ELISA were synthesized on a Symphony 12-channel multiplex peptide synthesizer (Protein Technologies, Tucson, AZ, USA) as C-terminal amides using standard instrument coupling protocols, or ordered from Mimotopes (Clayton, VIC, Australia). Titertek 96-well polyvinylchloride (PVC) microplates were from MP Biomedicals (Seven Hills, NSW, Australia). DPBS (1 \times) and goat anti-mouse IgG(H+L)-FITC conjugate (Zymed) were from Life Technologies (Mulgrave, VIC, Australia). Pyrochrome chromogenic reagent, Glucashield Buffer (β -glucan inhibiting buffer), Control standard endotoxin (CSE) *Escherichia coli* 0113:H10, and endotoxin free plasticware were from Associates of Cape Cod (East Falmouth, MA, USA). LAL reagent water, and pyrogen free test tubes were from Lonza (Mt Waverley, VIC, Australia). All other reagents were purchased from Sigma-Aldrich (Castle Hill, NSW, Australia) at the highest available purity.

Equipment. Deionized double distilled H₂O (ddH₂O) was used throughout and was

prepared by a Millipore Simplicity UV ultrapure water system. Microwave-assisted manual peptide synthesis was performed on a CEM Discover SPS Microwave Peptide Synthesizer (CEM, Matthews, NC, USA). Cell lysis was performed using a Branson Sonifier 450A analog ultrasonic cell disruptor. Electrospray ionization-mass spectrometry (ESI-MS) was performed on a Perkin Elmer-Sciex API3000 triple quadrupole instrument using Analyst 1.4 software (Applied Biosystems-MDS Sciex, Framingham, MA, USA). Protein masses were reconstructed using BioAnalyst 1.5.1 software (AB Sciex, Framingham, MA, USA). ^1H and ^{13}C -NMR spectra were recorded on a Bruker Avance 300 or 500 MHz spectrometers (Bruker Biospin, Germany) at 298 °K. Chemical shifts are reported in parts per million (ppm) downfield from tetramethylsilane. NMR spectra were processed using Topspin software (Bruker Biospin, Germany). UV-Vis spectroscopy was performed on a Cary 50 Bio Spectrophotometer with Cary WinUV Software (Varian Inc, Palo Alto, CA, USA). Dynamic light scattering (DLS) particle size analysis was acquired on a Zetasizer Nano ZS (Malvern Instruments, Worcestershire, UK) at 25 °C using disposable cuvettes. Transmission electron microscopy (TEM) was performed on a JEOL-1010 instrument (JEOL Ltd, Japan) operating at an accelerating voltage of 100 kV. Samples were applied to glow discharged carbon coated 200 mesh grids for 3 min, and then wicked off with filter paper. Microplate assays were read on a SpectraMAX 190 plate reader with SoftMax Pro software (Molecular Devices, Sunnyvale, CA, USA). DNA sequencing was performed by the Australian Genome Research Facility (AGRF; Brisbane Node, the University of Queensland) on an Applied Biosystems 3730xl DNA analyzer using ABI Prism BigDye terminator sequencing chemistry (version 3.1). Confocal Microscopy was performed on a Zeiss LSM 510 META confocal scan head mounted on an Axioplan 2 imaging platform (Carl Zeiss, Jena, Germany). Data was acquired using AIM 4.2 LSM software (Carl Zeiss).

Analytical reversed-phase high-performance liquid chromatography (RP-HPLC) was performed using a Shimadzu Prominence Analytical HPLC system (SIL-20AC HT autosampler, SPD-M10A Vp diode array detector, DGU-20A5 degasser, LC-20AB binary solvent delivery unit, CBM-20Alite card-type system controller, and Labsolutions 5.32 SP1 software). Preparative RP-HPLC was performed using a Shimadzu Preparative HPLC system (2 × LC-20AP large-scale preparative solvent delivery units, SPD-20A UV-Vis detector, FRC-10A fraction collector, CBM-20A system controller, 3725i-038 Rheodyne preparative scale manual sample injector, and Labsolutions 5.42 SP3 software). Separations were performed in gradient mode over 30 min for analytical, and 60 min for preparative separations. Solvent A consisted of 0.1 % (v/v) TFA in H_2O . Solvent B consisted of 90 % (v/v) MeCN/0.1 % (v/v) TFA in H_2O . Separation was achieved on C4 stationary phases, except for the GAS-Cys polytope, which was separated on a C18 stationary phase. The following columns (300 Å pore size) were used: 1) Vydac C4 analytical (214TP54; 250 × 4.6 mm; 5 μm), 2) Vydac C18 analytical (218TP54; 250 × 4.6 mm; 5 μm), 3) Vydac C4 preparative (214TP1022; 250 × 22 mm; 10 μm), and 4) Vydac C18 preparative (218TP1022; 250 × 22 mm; 10 μm). A flow-rate of 1 mL/min or 10 mL/min was used for analytical or preparative scale separations respectively, with detection at 214 nm for analytical and 230 nm for preparative runs.

6-Maleimidohexanoic Acid Synthesis. The synthesis was performed as described by de Figueiredo, *et al*¹ with modifications. Maleic anhydride (5 g; 51 mmol) and

aminohexanoic acid (6.7 g; 51 mmol) were refluxed (silicon oil bath, 170 °C) in dry glacial AcOH (40 mL) for 90 min. The reaction was cooled to RT, and the solvent removed by rotary evaporation. Residual AcOH was removed by coevaporation with toluene. The remaining residue was taken up in EtOAc (300 mL), washed with ddH₂O (3 x 100 mL), then saturated aqueous NaCl (50 mL), dried (MgSO₄), filtered, and concentrated. The mixture was purified on a 10 (h) × 10 (d) cm silica plug column, eluted with 1:4 hexane-EtOAc, concentrated, dissolved in boiling EtOAc, and recrystallized by dropwise addition of hexane to give 6-maleimidohexanoic acid (5.2 g; 48 % yield) as a white powder. Characterization data matched that reported in the literature.¹

¹H-NMR (300 MHz; CDCl₃): δ 6.69 (2H, s), 3.52 (2H, t), 2.35 (2H, t), 1.56-1.70 (4H, m), 1.3-1.37 (2H, m).

ESI-MS: [2M+H]⁺ *m/z* 423.5 (calcd. 423.4), [M+H]⁺ *m/z* 212.2 (calcd. 212.2). MW 211.21 g/mol.

TLC: R_f 0.55 (1:4 Hexane-EtOAc)

2-Acetyldimedone (Dde-OH) Synthesis. DCC (33.9 g; 164 mmol), DMAP (20.0 g; 164 mmol), and AcOH (9.9 g; 164 mmol) were added to a stirred suspension of dimedone (23 g; 164 mmol) in DCM (200 mL). The reaction was protected from light, and stirred for 16 h at RT. The reaction mixture was filtered, concentrated, taken up in EtOAc (200 mL), and washed with 5 % (v/v) HCl (3 x 100 mL), and saturated aqueous NaCl (50 mL). The organic phase was dried (MgSO₄), filtered, and concentrated. The mixture was purified on a 10 (h) × 10 (d) cm silica plug column, eluting with hexane and concentrated to give Dde-OH (21.6 g; 73 % yield) as yellow crystals. Characterization data matched that reported in the literature.²

¹H-NMR (300 MHz; CDCl₃): δ 2.59 (3H, s, CH₃), 2.51 (2H, s, CH₂), 2.36 (2H, s, CH₂), 1.10 (6H, s, C(CH₃)₂).

ESI-MS: [M+H]⁺ *m/z* 183.4 (calcd. 183.2). MW 182.22 g/mol.

TLC: R_f 0.5 (2:3 EtOAc-Hexane)

2-[[1-(4,4-dimethyl-2,6-dioxocyclohexylidene)ethyl]amino]-hexadecanoic acid (Dde-C16-OH) Synthesis. To 2-Aminohexadecanoic acid hydrochloride (10 g; 32.5 mmol) and Dde-OH (6.5 g; 35.7 mmol; 1.1 eq) in EtOH (200 mL) was added TEA (9.86 g; 97.4 mmol; 3 eq). The mixture was refluxed (silicon oil bath, 150 °C) for 2 days, and subsequently cooled to RT. The reaction was filtered, concentrated (rotary evaporation), taken up in EtOAc (200 mL), and then washed with 5 % (v/v) HCl (3 x 100 mL), and saturated aqueous NaCl (50 mL). The organic phase was dried (MgSO₄), filtered, and concentrated (rotary evaporation) to give a yellow gum, which was purified on a 10 (h) × 10 (d) cm silica plug column. The product was eluted using a stepwise gradient (1:4 EtOAc-hexane to 100 % EtOAc) and concentrated to give Dde-C16-OH (10.5 g; 67 % yield) as a white powder. Characterization data matched that reported in the literature.²

¹H-NMR (400 MHz; CDCl₃): δ 4.38 (1H, m, α-CH), 2.54 (3H, s, CH₃CNH), 2.41 (4H, s, 2 x CH₂CO), 2.01-1.88 (2H, m, β-CH₂), 1.45-1.20 (24H, m, 11 x CH₂), 1.04 (6H, s, C(CH₃)₂), 0.87 (3H, t, CH₃).

ESI-MS: [M+H]⁺ *m/z* 436.8 (calcd. 436.6). MW 435.64 g/mol.

TLC: R_f 0.43 (90:8:2 CHCl₃-MeOH-AcOH)

Peptide Synthesis. Peptides **2** and **3** were synthesized using a combination of manual solid-phase peptide synthesis (SPPS) and microwave assisted SPPS using HBTU (or HATU) for Dde-16-OH/DIPEA *in situ* neutralization³ and Fmoc-chemistry on rink amide MBHA resin (0.59 mmol/g). Before commencing peptide synthesis, the resin was swollen in DMF (10 mL/g resin) for 2 h, with an Fmoc-deprotection step performed prior to coupling the first amino acid. Fmoc-deprotection was achieved by 3 × 5 min treatments with 20 % (v/v) piperidine-DMF for manual synthesis steps, or 2 × 5 min treatments at 60 °C for microwave assisted synthesis. Dde-deprotection was achieved by multiple 10 min treatments with 2 % (v/v) hydrazine hydrate in DMF. To ensure complete Dde-removal, UV monitoring at 300 nm was performed until no change in absorbance was observed. This typically required approximately 4 × 10 min treatments. After Fmoc and Dde deprotection steps, a 1 min DMF flow wash was performed, followed by 30-60 min couplings with 4 eq of preactivated amino acid for manual couplings. Microwave assisted couplings were assembled as per manual couplings, and performed for 5 min at 70 °C with dynamic heat control. Histidine and cysteine residues were coupled for 10 min at 50 °C to minimize racemization.⁴ Acceleration of arginine γ -lactam formation occurs under microwave coupling conditions, reducing the concentration of activated arginine available to participate in peptide chain elongation. To minimize arginine deletion products a modified double coupling protocol from CEM was used (first coupling: 25 min at 25 °C, then 70 °C for 5 min; second coupling: 70 °C for 5 min).⁵ Amino acid activation was achieved by dissolving amino acids (4 eq) in 0.5 M HBTU or HATU-DMF solution (3.92 eq) to which DIPEA (5.68 eq) was added. Amino acids (except Fmoc-His(Trt)-OH) were preactivated for 1 min prior to their addition to the resin. Coupling yields were determined by the quantitative ninhydrin test⁶ for steps performed at RT. Where necessary, couplings were repeated to ensure coupling yields greater than 99.7 %. For microwave-assisted coupling steps amino acids were routinely double-coupled. Fmoc-amino acids with the following side-chain protection were used: Arg(Pbf), Asn(Trt), Gln(Trt), Glu(tBu), His(Trt), Lys(Boc), Ser(tBu), Thr(tBu), Tyr(tBu).

Peptides **2** and **3** were synthesized from a common resin-bound lipid adjuvant species. This compound was synthesized using manual SPPS (0.5 mmol scale). HATU was used for Dde-16-OH couplings, and HBTU for all other coupling steps. The lipid adjuvant sequence was assembled by coupling Fmoc-Gly-OH, followed by two copies of Dde-C16-OH, Fmoc-Gly-OH, and Dde-C16-OH. A di-lysine spacer, to mimic the spacing observed in the Lipid-Core Peptide (LCP) system, was then attached using two copies of Fmoc-Lys(Boc)-OH. The resin was then split into two 0.2 mmol batches. The DCpep (**2**; FYPSYHSTPQRP) or CONTROLpep (**3**; EPIHPETTFTNN) sequences were then attached using microwave assisted peptide synthesis, and 6-maleimidohexanoic coupled to the N-terminus of each peptide using standard coupling conditions for 1 h at RT. The resins were subsequently washed with DMF × 3, DCM × 3, dried overnight in a desiccator (under vacuum), and cleaved using 95:2.5:2.5 TFA-triisopropylsilane-H₂O (10 mL/g resin). Following removal of the cleavage cocktail using a high vacuum rotary evaporator at RT, the peptides were precipitated with ice-cold diethyl ether, pelleted by centrifugation (5 k ×g, 10 min, RT), dissolved in 40 % (v/v) aqueous MeCN containing 0.1 % (v/v) TFA, filtered, and lyophilized. The peptides were purified by RP-HPLC (60 % solvent B for 5 min, then 60-90 % solvent B over 60 min) on a preparative C4 column to yield peptides **2** and **3**.

Peptide Analytical Data.

Peptide 2. Yield: 43 %; HPLC: t_R = 11.3 min (60-90 solvent B, C4), 25.7 min (0-100 solvent B, C4); Purity: > 99 %; ESI-MS: m/z [M+2H]²⁺ 1402.3 (calcd. 1402.3), [M+3H]³⁺ 935.2 (calcd. 935.2), [M+4H]⁴⁺ 701.6 (calcd. 701.7), m/z 2802.8 (reconstructed); MW 2802.5 g/mol.

Peptide 3. Yield: 38 %; HPLC: t_R = 14.8 min (60-90 solvent B, C4), 26.9 min (0-100 solvent B, C4); Purity: > 99 %; ESI-MS: m/z [M+2H]²⁺ 1362.7 (calcd. 1362.2), [M+3H]³⁺ 908.5 (calcd. 908.5), m/z 2723.4 (reconstructed); MW 2722.4 g/mol.

PCR-based Gene Synthesis⁷ to Generate GAS Polytope Gene. The polytope protein sequence (Table S1) was designed to incorporate: 1) a thrombin cleavable N-terminal hexahistidine tag, 2) seven GAS M protein N-terminal peptide sequences,⁸ 3) a sequence from the conserved C-terminal GAS M protein segment (p145, underlined) fused with yeast GCN4 sequences to promote helicity (yielding the J14 peptide),⁹ and 4) a PADRE1024.03 universal T-helper epitope¹⁰ (sequences in Table S1). A di-lysine spacer was used to separate each component. The sequence was reverse translated and codon optimized for *E. coli* using the DNAsworks server (<http://helixweb.nih.gov/dnaworks/>), followed by the manual addition of restriction sites (5'-NdeI and 3'-SapI) (Table S2; as described in the NEB Impact Kit manual) to allow for restriction/ligation cloning into pTXB1 (NEB). Overlapping oligonucleotides (Table S3) for PCR-based gene synthesis (\leq 60 bp length) were designed using assembly PCR oligomaker (http://publish.yorku.ca/~pjohnson/Assembly_PCRoligomaker.html), and ordered from IDT with standard desalting. The oligonucleotides were individually dissolved in PCR grade water to 100 μ M, and used to produce an internal oligonucleotide stock solution (F2-9 & R1-8; 5 μ M/oligonucleotide).

The PCR-based gene synthesis reaction was assembled using 10 \times KOD polymerase buffer #1 (5 μ L; 1 \times), 2 mM dNTPs (5 μ L; 0.2 mM), 25 mM MgCl₂ (3 μ L; 1.5 mM), 5 μ M internal oligonucleotide stock (0.2 μ L; 20 nM/oligonucleotide), 100 μ M external (F1 & R9) oligonucleotides (0.2 μ L; 0.4 μ M/oligonucleotide), and water to 50 μ L. KOD DNA polymerase (2.5 U/ μ L; 0.4 μ L; 1 U) was added. The reaction was denatured at 98 °C (15 sec), and then subjected to 25 cycles of 98 °C (15 sec), 50 °C (2 sec), and 72 °C (20 sec). The PCR product was purified using a QIAquick PCR purification kit, and eluted with water.

Restriction-Free Cloning to Generate pTXB1_GAS polytope_GyrA Vector. The GAS polytope gene was inserted into pTXB1 using a restriction-free overlap extension PCR approach as described.¹¹ Chimeric PCR primers (Table S2; RF series) were designed with 5'-ends that can anneal to the pTXB1 plasmid (Table S2; underlined) and 3'-ends that can anneal to the GAS polytope gene. The GAS polytope gene synthesis product was amplified by PCR using these primers and Phusion DNA polymerase to generate a linear product (a megaprimer) containing sequences from the pTXB1 plasmid at either end (Table S2). This product was gel purified and used in a second PCR reaction (10 μ L volume; 18 cycles; 5 ng of pTXB1, 67 ng megaprimer (250 eq), Phusion DNA polymerase, and 3 % (v/v) DMSO) to incorporate the insert into the vector. Subsequently DpnI (0.5 μ L; 20 U/ μ L; 10 U) was added to the reaction mixture, and incubated at 37 °C for 1 hour to destroy the

parental plasmid. This mixture (5 μ L) was used to transform 50 μ L of ultra-competent (Inoue method) DH5 α *E. coli* by heat shock. The plasmid (pTXB1_GAS polytope_GyrA) was purified using a QIAprep spin minikit and sequenced.

Site-Directed Mutagenesis to Generate pTXB1_GAS polytope-Cys Vector. The pTXB1_GAS polytope-Cys vector was generated from pTXB1_GAS polytope_GyrA using the QuikChange XL II site-directed mutagenesis kit according to the manufacturers instructions. Primers (Table S2, Stop-For and Stop-Rev) were designed using the QuikChange Primer Design program (www.genomics.agilent.com). These primers were designed to convert an ATC (Ile) codon (3' to the pTXB1 *Mxe* GyrA intein N-terminal TGC (Cys) codon) to an amber stop codon (TAG).

Expression of the GAS-Cys Polytope Protein 1. The pTXB1-polytope-Cys vector was transformed into competent BL21-codonplus (DE3)-RIL *E. coli* by heat shock, and grown to OD₆₀₀ 0.6 at 37 °C, 250 RPM in LB (Miller) broth containing 100 μ g/mL ampicillin and 34 μ g/mL chloramphenicol. Protein expression was induced with 0.5 mM IPTG, and the cells incubated for 4 hours at 37 °C, 250 RPM. The cells were pelleted (5 k \times g, 15 min, 4 °C), and lysed in denaturing lysis buffer (6 M guanidine-Cl, 500 mM NaCl, 20 mM Tris pH 8, 20 mM imidazole, 5 mM β -mercaptoethanol) by sonication (6 x 30 sec on, 2 min off) on ice. The mixture was cleared (30 k \times g, 20 min, RT). The expressed protein was purified from the supernatant using Ni-NTA beads. After binding for 1 h at 4 °C the beads were thoroughly washed with wash buffer (500 mM NaCl, 20 mM Tris pH 8, 20 mM imidazole, 5 mM β -mercaptoethanol), and PBS. The protein was eluted with 500 mM imidazole in wash buffer, and purified by HPLC (20 % solvent B for 5 min, then 20-50 % solvent B over 60 min) on a C18 preparative scale column. Pure fractions were combined, lyophilized, and characterized by reversed-phase HPLC and ESI-MS.

Conjugation of GAS Polytope and Lipid Adjuvants. Bioconjugation reactions were performed in maleimide conjugation buffer (6 M guanidine-Cl, 50 mM NaPi pH 7.3, 20 % (v/v) MeCN, 5 mM EDTA). Lipid adjuvant peptides **2** or **3** were dissolved in DMSO as a solubility enhancer (final concentration 4 % (v/v)). Alternatively DMF was used, however lower product yields were observed. Use of TCEP to maintain reduced cysteine thiols is discouraged due to reactivity with maleimide groups^{12, 13} in the lipid adjuvant peptides. The reaction was performed as described. Briefly, to 8 mg of GAS-Cys polytope protein **1** (327 nmol; \sim 80 μ M; \sim 2 mg/mL) dissolved in 4 mL maleimide conjugation buffer was added \sim 4.2 mg (\sim 4.7 eq; 1534 nmol; \sim 384 μ M) of lipid adjuvant peptide **2** or **3** dissolved in DMSO (160 μ L). The reaction was left to incubate at RT for 30 min and subsequently purified by HPLC (30 % solvent B for 5 min, then 30-100 % solvent B over 60 min) on a preparative C4 column to yield lipoprotein vaccine constructs **4** or **5** respectively. These constructs were characterized by analytical RP-HPLC and ESI-MS. Construct **4** was subjected to peptide mass fingerprinting after endoproteinase AspN digestion to provide evidence of site-specific conjugation, and to ensure the GAS-Cys polytope sequence is correct.

Thrombin Cleavage of the N-terminal Hexahistidine-Tag. Lipoproteins **4** or **5** (4.6 mg; \sim 168 nmol; \sim 1 mg/mL; \sim 37 μ M) were dissolved in DPBS (4.5 mL) with bath ultrasonication. Thrombin (human plasma; 30 U) was added, and the reaction incubated at RT for 3 h. The product was subsequently purified by HPLC (30 % solvent B for 5 min, then 30-90 % solvent B over 60 min) on a preparative C4 column

to yield lipoprotein vaccine constructs **6** or **7** respectively. These constructs were characterized by analytical RP-HPLC, ESI-MS, DLS, and TEM.

Protein Analytical Data. ESI-MS and RP-HPLC data for proteins is presented in Figure S1-S3. SDS-PAGE data is presented in Figure S4.

GAS-Cys Polytope Protein (1). HPLC: $t_R = 18.0$ min (0-70 % solvent B, C18), 16.8 min (20-50 % solvent B, C18), 12.9 min (0-100 % solvent B, C4); Purity: > 99 %; ESI-MS: m/z 24,504.4 (reconstructed); MW 24,498.9*.

Lipoprotein 4. Yield 71 %; HPLC: $t_R = 16.4$ min (30-90 % solvent B, C4), 20.7 min (0-100 % solvent B, C4); Purity: > 99.5 %; ESI-MS: m/z 27,300.0 (reconstructed); MW 27,301.4*.

Lipoprotein 5. Yield 89 %; HPLC: $t_R = 16.5$ min (30-90 % solvent B, C4), 20.7 min (0-100 % solvent B, C4); Purity: > 99.5 %; ESI-MS: m/z 27,219.9 (reconstructed); MW 27,221.3*.

* These constructs also contain a small amount of product missing the N-terminal alanine residue. This is due to cleavage of the initiator methionine by methionine aminopeptidase (MAP) followed by cleavage of the N-terminal alanine by MAP¹⁴ or another enzyme (e.g. PepN¹⁵).

Lipoprotein (Δ His₆) 6. Yield 89 %; HPLC: $t_R = 17.8$ min (30-90 % solvent B, C4), 21.7 min (0-100 % solvent B, C4); Purity: > 99 %; ESI-MS: m/z 25,311.3 (reconstructed); MW 25,313.4.

Lipoprotein (Δ His₆) 7. Yield 75 %; HPLC: $t_R = 17.9$ min (30-90 % solvent B, C4), 21.7 min (0-100 % solvent B, C4); Purity: > 99 %; ESI-MS: m/z 25,239.0 (reconstructed); MW 25,241.2.

Evidence for Site-Specific Maleimide Conjugation Reactions, and Peptide Mass Fingerprinting (PMF) of the GAS-Cys Polytope Sequence. To confirm that the conjugation reaction between lipid adjuvant peptide **2** or **3** and the GAS-Cys polytope **1** was site-specific, occurring only through the C-terminal cysteine residue, a PMF approach was taken. The enzyme endoproteinase Asp-N (cleaves N-terminally to Asp and cysteic acid) was selected, as it will not cleave within the lipid adjuvant peptide **2** sequence. The proteolytic species generated will therefore contain peptides incorporating fragments of protein **1** conjugated to **2**, which can be used to determine the conjugation site. Lipoprotein **4** (0.2 mg; ~7.3 nmol) was dissolved in 100 mM Tris pH 8 to 1 mg/mL (~ 36 μ M) with bath ultrasonication. To this mixture was added 2 μ L endoproteinase Asp-N (80 ng; 40 μ g/mL in 10 mM Tris-Cl pH 8; 1/2500 (w/w) enzyme to substrate ratio). The mixture was incubated at 37 °C for 18 hours and subsequently analysed by analytical RP-HPLC (0-100 % solvent B, C4; Figure S5, A) and LC-MS. All peaks were also subjected to offline ESI-MS analysis (to assign RP-HPLC chromatogram peaks) and mapped against a table of endoproteinase Asp-N cleavage products generated by PeptideCutter (http://www.expasy.org/peptide_cutter/). This analysis yielded 79.8 % coverage of the lipoprotein **4** sequence (see Figure S5, C). Information relating to the hydrophobicity of the proteolyzed peptides, obtained from the RP-HPLC chromatogram, was used to

investigate whether the maleimide conjugation reaction was site-specific. The lipid adjuvant peptide **2** is extremely hydrophobic, eluting at 25.7 min (0-100 % solvent B, C4). In comparison, lipoprotein 4 eluted at 20.7 min, and GAS-Cys polytope protein **1** eluted at 12.9 min. Based on this information, it would be expected that proteolytic peptides conjugated to lipid adjuvant **2** would elute after 20.7 min, since these peptides are significantly smaller than the full-length lipoprotein **4**, and thus would not be expected to reduce the hydrophobic nature of **2** to the same extent as **1**. Only one significant species was identified that eluted in this range (Peak L, 2.4 min in Figure S5, A). The mass of this species (whole peak; Figure S5, B) corresponded to the C-terminal Asp-N fragment (Figure S5, C; peak L) conjugated to **2**, strongly supporting that conjugation occurred specifically through the C-terminal cysteine residue.

Stock Solutions for Immunization. Lipoproteins **6** or **7**, and protein **1** were dissolved in 6 M Gdn-Cl, 0.1 M NaPi pH 7.5 and quantified by measuring A_{280} values, using extinction coefficients (**1**: $9970 \text{ M}^{-1} \text{ cm}^{-1}$; **6**: $12950 \text{ M}^{-1} \text{ cm}^{-1}$; **7**: $9970 \text{ M}^{-1} \text{ cm}^{-1}$) calculated by ExpASY ProtParam (<http://www.expasy.org/protparam>). Known amounts of each compound were analyzed by RP-HPLC (0-100 % solvent B, C4), and used to define the amount of protein per area under the curve (AUC) unit at 214 nm. This information was used to generate 0.6 mg/mL stock solutions of lipopeptide **6** or **7**, and a 1.2 mg/mL stock solution of protein **1** in $1\times$ DPBS (Gibco).

Endotoxin Testing. A Pyrochrome chromogenic *Limulus* amoebocyte lysate (LAL) endpoint assay (Associates of Cape Cod, East Falmouth, MA, USA) was performed to certify that endotoxin levels for lipoprotein **6** and **7** stock solutions were below pharmacopoeia limits (USP/BP). The endotoxin limit (EL) concentration was set at 1.2 IU/mL. This value was calculated using a minimal pyrogenic dose (K) of 0.06 IU/dose, and an administered volume per dose of 50 μL . The K value was calculated using a 5 IU/kg endotoxin limit for parenteral administration (USP/BP) and a 12 g minimal mass for 4-6 week old female mice (source: Jax mice). All consumables were certified endotoxin free. Assays were performed in 96-well polystyrene plates with lids, using 50 μL total sample volumes. All samples were tested to ensure their pH was 6-8 and that they do not absorb at 400-410 nm. The following groups were assessed: 1) LAL reagent water and PBS (negative controls), 2) control standard endotoxin standard curve (0.1-2 IU/mL), 3) lipoproteins **6** and **7** (experimental group), 4) positive lipoprotein control (lipoproteins **6** and **7** spiked with control standard endotoxin to 0.5 IU/mL). The positive lipoprotein control groups were performed to ensure that lipoproteins **6** or **7** do not inhibit/enhance the amount of endotoxin detected. The Pyrochrome LAL reagent was reconstituted with Glucashield buffer, which prevents (1,3)- β -D-glucan contamination from activating the LAL cascade, leading to false positive results. Reconstituted Pyrochrome LAL reagent was added to each sample (50 μL /well), and the reaction incubated at 37 $^{\circ}\text{C}$ until all the standard curve sample samples displayed a yellow color. At this point reactions were stopped with 50 % (v/v) acetic acid- H_2O (25 μL /well), and the OD_{405} value for each well was acquired using a microplate reader. Endotoxin levels were determined by comparison to the standard curve (OD_{405} against standard endotoxin concentrations).

Immunization and Blood Collection. Immunization was performed under protocols approved by the Griffith University (BDD/06/10/AEC) and University of Queensland (SCMB/GRIFITH/005/12/MERCK/NIH/NHF/NHMRC) animal ethics committees in

accordance with Australian National Health and Medical Research Council (NHMRC) guidelines. Proteins (**1**, **6**, and **7**) were produced as 0.6 mg/mL stock solutions. Lipoproteins **6** and **7** were administered in 1× DPBS, and protein **1** as a 1:1 emulsion with complete Freund's adjuvant (CFA; positive control). C57BL/6J mice (♀; 5 weeks old; 5/group; Animal Resources Centre, WA, Australia) were immunized subcutaneously at the tail base with 30 µg (50 µL) of each stock solution, or with 50 µL 1× DPBS (negative control), on days 0, 21, 28, and 35. On day 42, blood was collected from the tail vein, and left to clot for 1 h at 37 °C. Serum was collected after centrifugation (1000 ×g, 10 min, RT) and stored at -20 °C.

Enzyme-Linked Immunosorbent Assay (ELISA). ELISA was performed essentially as described, using sera from individual mice.⁹ Peptide antigen stock solutions (5 µg/mL) were made in carbonate coating buffer (66 mM bicarbonate/carbonate pH 9.6) and used to coat polyvinylchloride (PVC) 96-well microtiter plates (100 µL/well; 0.5 µg/well) at 4 °C for 16 hours. The antigen solutions were then removed, and the wells blocked with 5 % (w/v) skim milk in PBS-T (0.05 % (v/v) tween-20, PBS) (150 µL/well) at 37 °C for 1.5 h. The plates were thoroughly washed (3× ddH₂O, 2× PBS-T), and twofold serial dilutions of sera in 0.5 % (w/v) skim milk in PBS-T (starting at 1:100; 100 µL/well) produced. The plates were incubated at 37 °C for 1.5 h, washed (3× ddH₂O, 2× PBS-T), and incubated at 37 °C for 1.5 h with α-mouse IgG-HRP conjugate (1:3000 dilution in 0.5 % (w/v) skim milk in PBS-T; 100 µL/well). The plates were washed (3× ddH₂O, 2× PBS-T), *O*-phenylenediamine (OPD; SIGMAFAST™ OPD; 100 µL/well) added, and incubated for 30 min in the dark at RT. Optical density was read at 450 nm using a microplate reader. Antibody titers were defined as the lowest dilution with an OD₄₅₀ value greater than three standard deviations above the mean absorbance of control wells (sera from PBS immunized mice).

Statistics. Statistical comparison of antibody titers between groups was performed using a one-way analysis of variance (ANOVA) followed by a Tukey's multiple comparison post-hoc test. Mean and standard error of the mean (SEM; σ/\sqrt{n}) were calculated using standard formula. GraphPad Prism 4 was used for statistical analysis, with $P < 0.05$ considered to be significant.

Confocal Microscopy. Confocal microscopy was used to assess the capacity of murine antibodies elicited against **1** (primed with CFA) or **6** (administered in PBS) to bind cell surface M proteins from GAS serotypes represented by N-terminal M protein peptides included in our polytope constructs (88/30 (*emm97*), PL1 (*emm54*), NS1 (*emm100*), Y504S (*emm11*), BSA10 (*emm2.3*), NS27 (*emm91*), NS5 (*emm101*))¹⁶, or against pM1 (*emm1*)¹⁷ which contains the conserved M protein J14i¹⁸ epitope found in J14. The confocal microscope was calibrated for positive and negative samples using pM1 GAS and murine antisera raised against recombinant M1 protein (primed with CFA)¹⁹ as a positive control, or antisera from sham (PBS) immunized mice as a negative control. Murine antisera against recombinant arginine deiminase (ADI)¹⁹ (99 % conserved amongst serotypes) was used as an additional positive control for each strain.

Slides were prepared as described.²⁰ A colony of each GAS strain was grown overnight at 37 °C (without shaking) in Todd Hewitt broth (5 mL) supplemented with 1 % yeast extract (THBY) and 28 µM E-64 (to inhibit M protein proteolysis by SpeB).

The cultures were subsequently pelleted (3×10^8 g, 5 min, RT), washed ($2 \times$ PBS), and resuspended to $OD_{600} \sim 0.4$ in PBS. Each suspension (10 μ L) was dispensed into wax circles (~ 1.2 cm \varnothing ; ImmEdge pen, Vector Laboratories, USA) on polylysine slides (Erie Scientific, USA), spread, and left to air dry. Bacteria were fixed with 3 % (w/v) paraformaldehyde-PBS (10 min), washed (PBS, 10 min), and blocked with 3 % (w/v) bovine serum albumin (BSA)-PBS-T (150 μ L/sample, 37 $^{\circ}$ C, 30 min). For all subsequent steps, antibodies were diluted with 0.3 % (w/v) BSA-PBS. The slides were washed (PBS, 2×10 min), and GAS cell surface immunoglobulin binding sites blocked with a 1:200 dilution of human plasma IgG (10 mg/mL stock; Calbiochem; 150 μ L/sample, 37 $^{\circ}$ C, 1 h). After washing (PBS, 2×10 min), the slides were treated with a 1:200 dilution of pooled murine antiserum (final bleed; 150 μ L/sample, 37 $^{\circ}$ C, 1.5 h) from protein **1** (primed with CFA), lipoprotein **6** (1:50 dilution for Y504S and pM1), sham (PBS), recombinant M1 GAS M protein (primed with CFA), or recombinant ADI (primed with CFA) immunized mice. The slides were washed (PBS, 3×10 min) and incubated with a 1:200 dilution of FITC-labeled secondary antibody (goat anti-mouse IgG-FITC conjugate, Zymed, USA; 150 μ L/sample, 4 $^{\circ}$ C, overnight). After washing (PBS, 3×10 min), Vectashield Hardset mounting medium (7.5 μ L/sample; Vector Laboratories, USA) was applied to adhere glass coverslips. Confocal images were acquired using a Plan-Apochromat 100 \times /1.40 oil immersion DIC objective lens and Argon/2 laser with excitation at 488 nm for FITC. Filter sets were configured for detection of FITC. Brightfield DIC images were acquired to demonstrate the presence of bacteria for negative control experiments.

Table S1. The sequence of the designed polytope protein, each of the GAS M protein N-terminal peptide antigens, and the PADRE1024.03 universal T helper epitope.

Name	Sequence
Polytope (Designed)	HHHHHHGSGLVPRGKKKQAEDKVKASREAKKQVEKALEQLEDKVKKKDNGK AIYERARERALQELGPKKEVLTRRQSQDPKYVTQRISKKRVTTTRSQAQDAA GLKEKADKKTEVKAAGQSAPKGTNVSADLKKNSKTPAPAPAVPVKKEATKS KLSEAEHLHKKADDHPGAVAARNDVLSGFSKKADHPSYTAAKDEVLSHFVSVK KAKFVAAWTLKAAA
Polytope (Expressed)	ASSRVHHHHHHGSGLVPRGKKKQAEDKVKASREAKKQVEKALEQLEDKVKK KDNGKAIYERARERALQELGPKKEVLTRRQSQDPKYVTQRISKKRVTTTRSQ AQDAAGLKEKADKKTEVKAAGQSAPKGTNVSADLKKNSKTPAPAPAVPVK EATKSKLSEAEHLHKKADDHPGAVAARNDVLSGFSKKADHPSYTAAKDEVLS HFSVKKAKFVAAWTLKAAA
GAS M protein Conserved Peptide Epitopes	
J14	KQAEDKVKASREAKKQVEKALEQLEDKVK
GAS M Protein N-terminal Peptide Epitopes	
88/30 ₁₋₂₀ (<i>emm97</i>)	DNGKAIYERARERALQELGP
PL1 ₁₋₁₉ (<i>emm54</i>)	EVLTRRQSQDPKYVTQRIS
NS1 ₁₋₁₉ (<i>emm100</i>)	RVTTTRSQAQDAAGLKEKAD
Y504S ₁₋₂₀ (<i>emm11</i>)	TEVKAAGQSAPKGTNVSADL
BSA10 ₁₋₂₈ (<i>emm2.3</i>)	NSKTPAPAPAVPVKKEATKSKLSEAEHL
NS27 ₁₋₁₉ (<i>emm91</i>)	ADDHPGAVAARNDVLSGFS
NS5 ₁₋₁₉ (<i>emm101</i>)	ADHPSYTAAKDEVLSHFVSV
Universal Helper T Cell Epitope	
PADRE1024.03	AKFVAAWTLKAAA

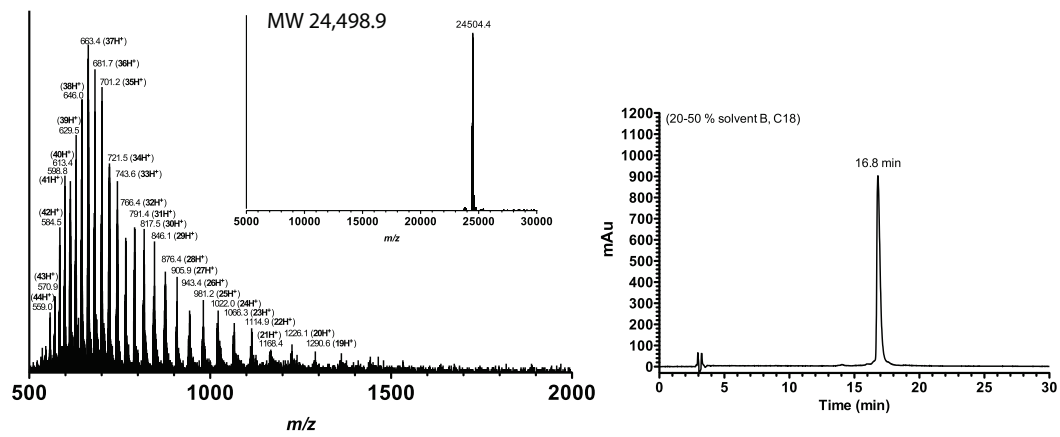
Table S2. The sequence of a) the codon-optimized polytope gene, with 5'-NdeI and 3'-SapI restriction sequences added (underlined), b) the polytope megaprimer (underlined portions anneal to pTXB1 vector), and c)

Name	Sequence
a) Polytope (PCR-based gene synthesis product)	<p>GGGAATTCCA/TATGCATCACCACCATCATCACGGGAGCGGCCTGGTGCCGCTGGCAAGAA GAAACAGGCGGAAGATAAAGTGAAGGCGAGCCGTGAAGCGAAAAACAGGTGGAGAAAACAC TGGAGCAACTGGAGGATAAGGTTAAGAAAAAGATAACGGCAAAGCGATTTATGAACGTGCG CGTGAACGGGCGCTGCAGGAATTAGGCCCGAAAAAGGAAGTCCTGACCCGTGTCAGAGCCA GGATCCGAAATATGTGACCCAGCGTATTAGCAAGAAACGTGTGACAACCCGTAGCCAGGCGC AGGATGCAGCCGGGTTGAAAGAAAAGGCAGATAAAAAAGACCGAAGTGAAGCGGCAGGCCAG AGCGCGCTAAAGGCACAAATGTGAGCGCGGACTTAAAAAGAACAGCAAAACTCCGGCTCC TGCTCCGGCGGTGCCGGTCAAGAAGGAGGCGACTAAAAGCAAAC TGAGCGAAGCGGAAC TGC ATAAGAAAGCCGATGACCACCCAGGTGCGGTGCGTGCCTGTAATGATGTGCTGAGCGGTTTT TCCAAAAGGCTGATCACCCAGCTACACTGCGGCGAAGGATGAAGTACTGAGCCATTTTAG CGTCAAAAAGCTAAGTTTGTGGCTGCGTGGACCCTTAAAGCAGCGGCG/TGCGGAAGAGCC TCGAG</p>
b) Megaprimer	<p>GGAGATATACATATGGCTAGCTCGCGAGTCCATCACCACCATCATCACGGGAGCGGCCTGGT GCCGCGTGGCAAGAAGAAAACAGGCGGAAGATAAAGTGAAGGCGAGCCGTGAAGCGAAAAAC AGGTGGAGAAAAGCACTGGAGCAACTGGAGGATAAGGTTAAGAAAAAGATAACGGCAAAGCG ATTTATGAACGTGCGGTGAACGGGCGCTGCAGGAATTAGGCCCGAAAAAGGAAGTCCTGAC CCGTGTCAGAGCCAGGATCCGAAATATGTGACCCAGCGTATTAGCAAGAAACGTGTGACAA CCCGTAGCCAGGCGCAGGATGCAGCCGGGTTGAAAGAAAAGGCAGATAAAAAAGACCGAAGTG AAAGCGGCAGGCCAGAGCGCGCTAAAGGCACAAATGTGAGCGCGGACTTAAAAAGAACAG CAAACTCCGGCTCCTGCTCCGGCGGTGCCGGTCAAGAAGGAGGCGACTAAAAGCAAAC TGA GCGAAGCGGAAC TGCATAAGAAAGCCGATGACCACCCAGGTGCGGTGCGTGCCTGTAATGAT GTGCTGAGCGGTTTTTCCAAAAGGCTGATCACCCAGCTACACTGCGGCGAAGGATGAAGT ACTGAGCCATTTTAGCGTCAAAAAGCTAAGTTTGTGGCTGCGTGGACCCTTAAAGCAGCGG CGTGATCACGGGAGATGCACTAGTTGCCCTA</p>

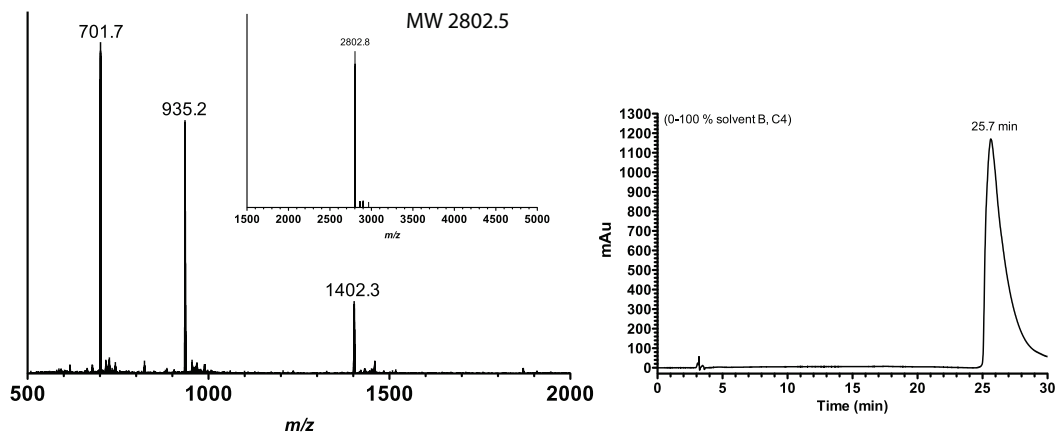
Table S3. Primers for PCR-based gene synthesis (F and R series) of the GAS polytope, restriction-free cloning (RF series; underlined portion anneals to vector), and generation of C-terminal cysteine by site-directed mutagenesis (Stop series; stop codon in bold).

Name	Sequence (5'→3')
F1	GGGAATTCATATGCATCACCACCATCATCACGGGAGCGGCCTGG
F2	AGGCGGAAGATAAAGTGAAGGCGAGCCGTGAAGCGAAAAACAGGTGGAGAAAGCACTG
F3	GATAAGGTTAAGAAAAAGATAACGGCAAAGCGATTTATGAACGTGCGCGTGAACGGGCG
F4	GGAAGTCCTGACCCGTCGTGAGAGCCAGGATCCGAAATATGTGACCCAGCGTATTAGCA
F5	GTAGCCAGGCGCAGGATGCAGCCGGGTTGAAAGAAAAGGCAGATAAAAAGACCGAAG
F6	CGCGCCTAAAGGCACAAATGTGAGCGCGGACTTGAAAAAGAACAGCAAAACTCCGGC
F7	GGTCAAGAAGGAGGCGACTAAAAGCAAACAGAGCGAAGCGGAACTGCATAAGAAAAGC
F8	GGTCGCTGCCCGTAATGATGTGCTGAGCGGTTTTTCCAAAAGGCTGATCACCCAG
F9	GATGAAGTACTGAGCCATTTAGCGTCAAAAAGCTAAGTTTGTGGCTGCGTGGACCC
R1	CCTTCACTTTATCTTCCGCCGTGTTTCTTCTTGCCACGCGGCACCAGGCCGCTCCCG
R2	TTTGCCGTTATCTTTTTTCTAACCTTATCCTCCAGTTGCTCCAGTGCTTCTCCACCTGTTT
R3	GACGGGTCAGGACTTCCTTTTTTCGGGCCATAATCCTGCAGCGCCCGTTCACGC
R4	CCTGCGCCTGGCTACGGGTTGTCACACGTTTCTTGCTAATACGCTGGGTCACATATTTT
R5	GTGCCTTTAGGCGCGCTCTGGCCTGCCGCTTCACTTCGGTCTTTTTATCTGCCTTTT
R6	CGCCTCCTTCTTGACCGGCACCGCCGGAGCAGGAGCCGGAGTTTTGCTGTTCTTTTT
R7	TCATTACGGGCAGCGACCGCACCTGGGTGGTCATCGGCTTCTTATGCAGTCCGCTT
R8	GCTAAAATGGCTCAGTACTTCATCCTTCGCCGAGTGTAGCTGGGGTGATCAGCCTTTTT
R9	CTCGAGGCTCTTCCGCACGCCGCTGCTTTAAGGGTCCACGCAGCCAC
RF-For	GGAGATATACATATGGCTAGCTCGCGAGTCCATCACCACCATCATCACGGGAGC
RF-Rev	TAGGGCAACTAGTGCATCTCCCGTGATGCACGCCGCTGCTTTAAGGGTCCA
Stop-For	CTTAAAGCAGCGCGTGCT TAG ACGGGAGATGCACTAGTT
Stop-Rev	AACTAGTGCATCTCCCGT CTAG CACGCCGCTGCTTTAAG

A. GAS-Cys Polytope Protein 1



B. Peptide 2



C. Peptide 3

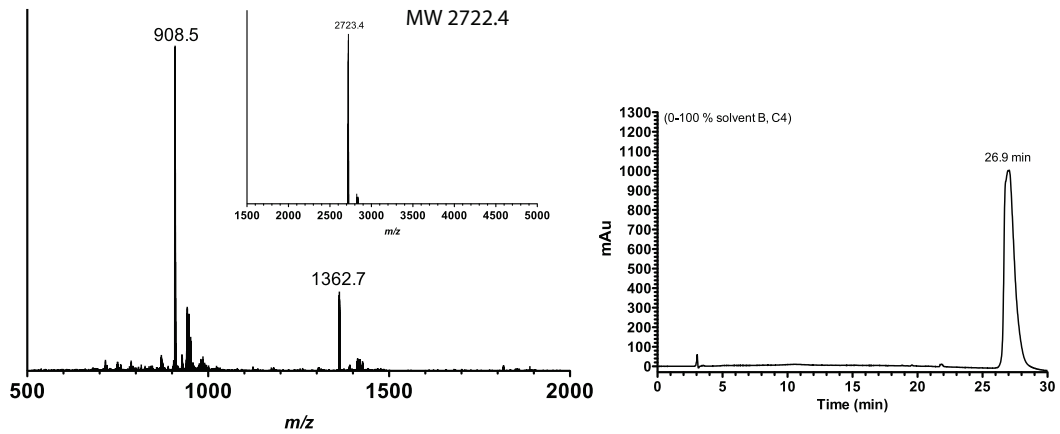
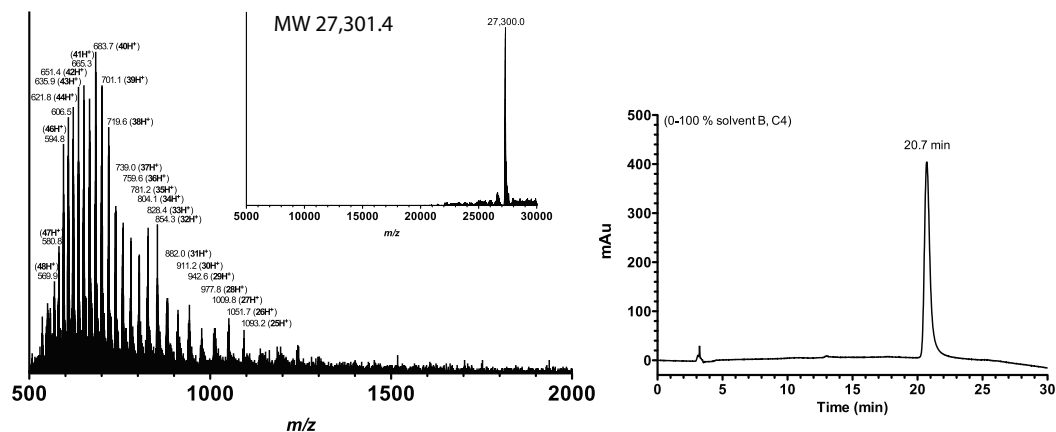


Figure S1. ESI-MS and RP-HPLC data for (A) polytope protein 1, (B) lipid adjuvant 2, and (C) lipid adjuvant 3.

A. Lipoprotein 4



B. Lipoprotein 5

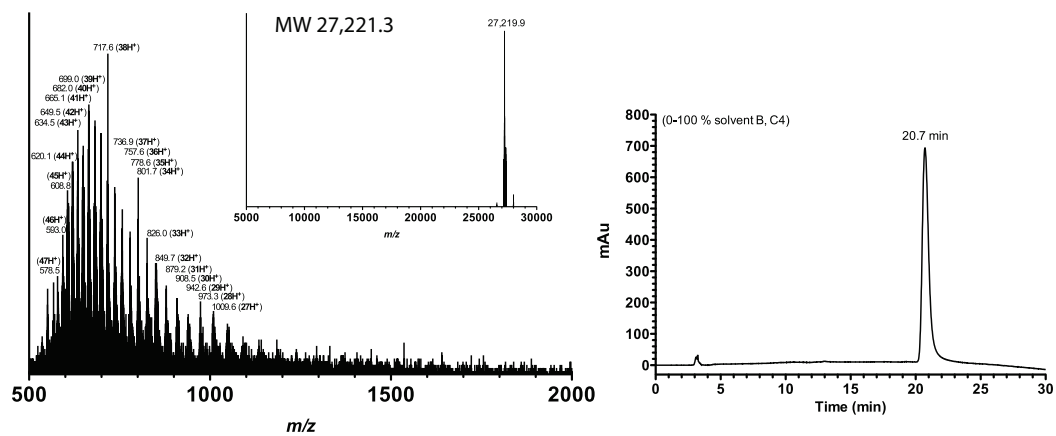
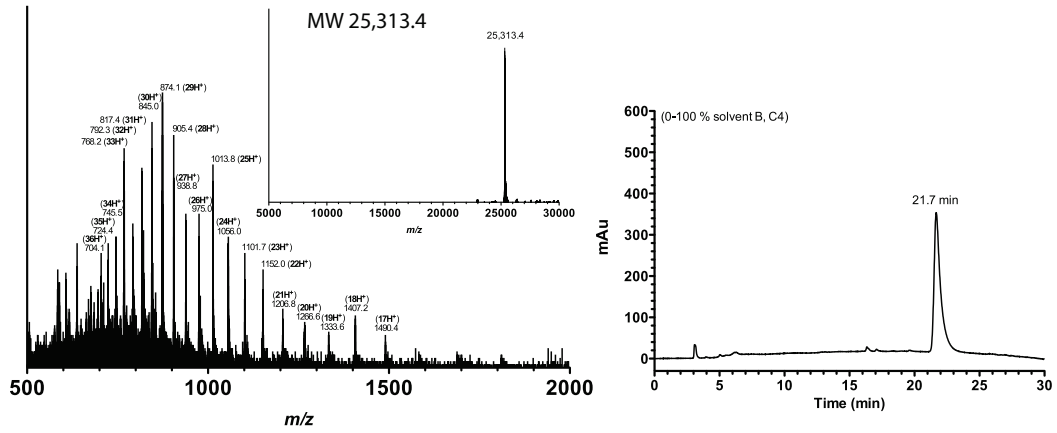


Figure S2. ESI-MS and RP-HPLC data for (A) lipoprotein 4 and (B) lipoprotein 5.

A. Lipoprotein 6



B. Lipoprotein 7

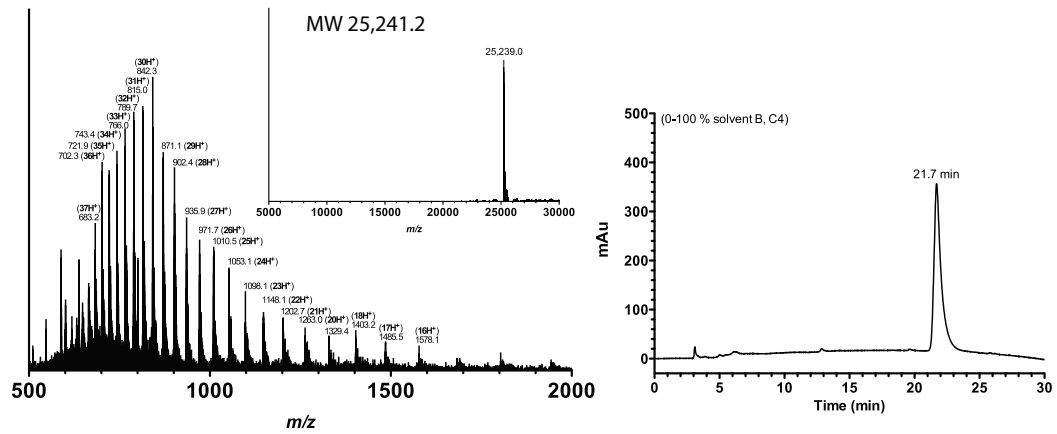


Figure S3. ESI-MS and RP-HPLC data for (A) lipoprotein 6 and (B) lipoprotein 7.

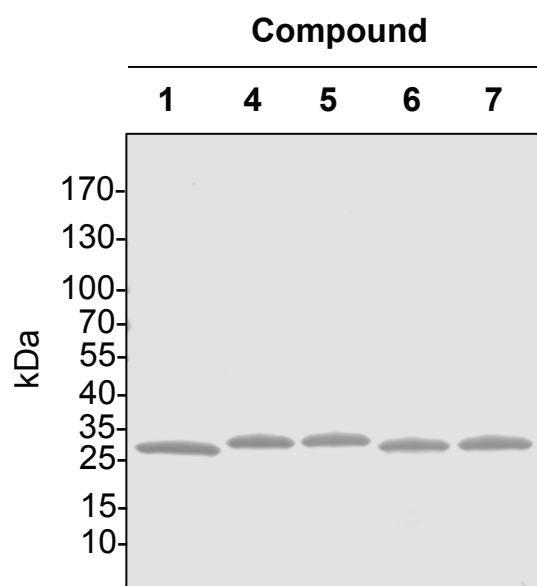


Figure S4. SDS-PAGE (4-12 % Biorad Mini-PROTEAN TGX) of protein products, stained with Coomassie R-250.

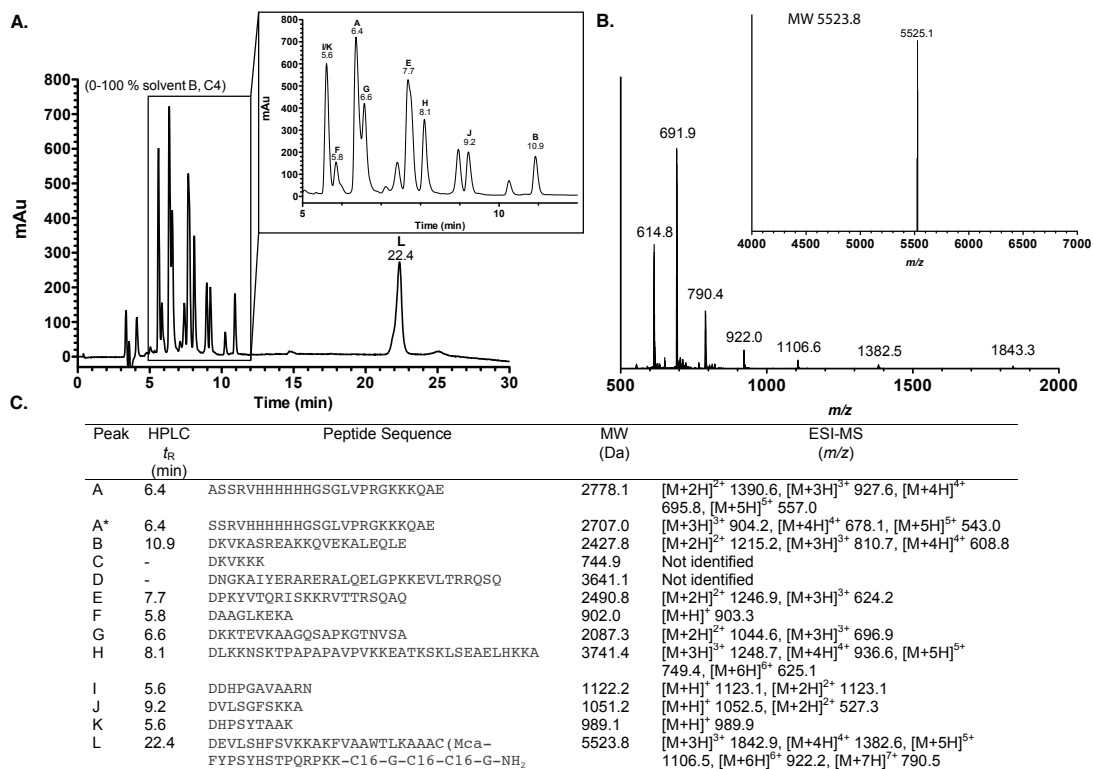


Figure S5. Peptide mass fingerprinting data (ESI-MS and RP-HPLC) for lipoprotein 4 after digestion with endoproteinase Asp-N. **(A)** RP-HPLC chromatogram of Asp-N digest reaction. **(B)** ESI-MS data for peak L (22.4 min) corresponding to the C-terminal polytope Asp-N digest peptide conjugated to peptide 2. **(C)** Table of expected Asp-N digest peptides and corresponding identified HPLC peaks and ESI-MS data.

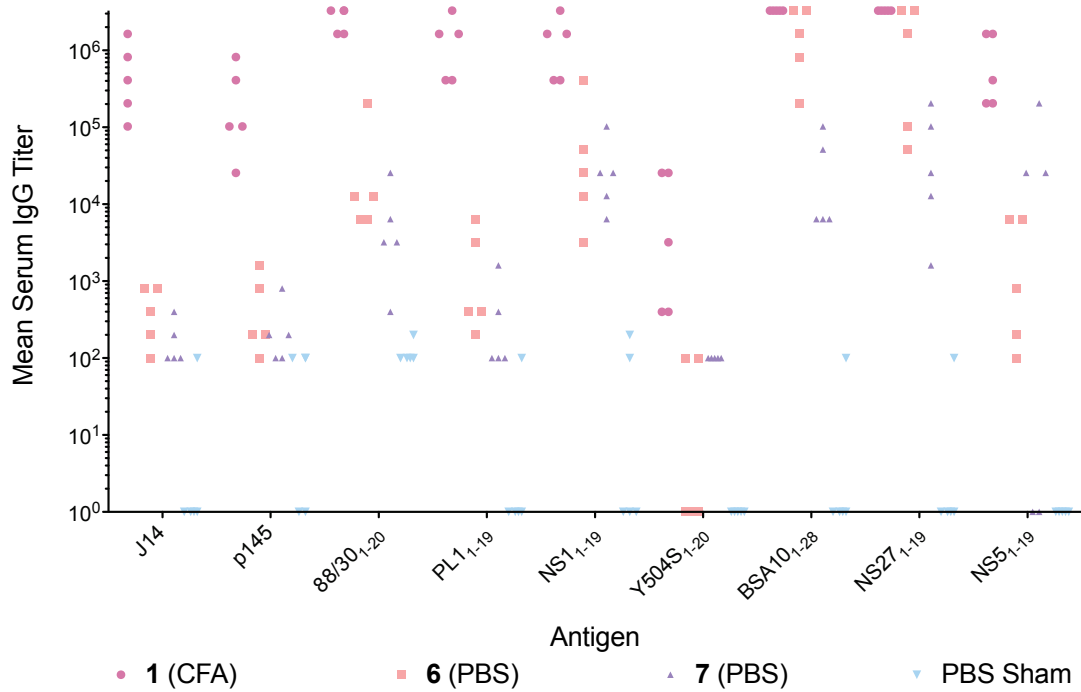


Figure S6. Assessment of antigen-mediated immunity elicited in response to immunization with recombinant antigen **1** (primed with CFA), lipoprotein **6** (includes DCpep) or **7** (includes CONTROLpep), or PBS sham (negative control). An ELISA was used to measure the mean antigen-specific serum IgG antibody titers (log₁₀), against the eight polytope antigens, from sera collected one-week after the final boost. Plates were coated with synthetic peptide antigens. The capacity for antibodies against J14 to bind the folded J14i conformational epitope was demonstrated using p145. Data is represented as scatterplots for each antigen group (n = 5), with mice that did not respond to immunization indicated by points on the x-axis.

References:

1. de Figueiredo RM, Oczipka P, Frohlich R, Christmann M. Synthesis of 4-maleimidobutyric acid and related maleimides. *Synthesis* 2008;**Synthesis**:1316-8.
2. Ross BP, Falconer RA, Toth I. N-1-(4,4-dimethyl-2,6-dioxocyclohex-1-ylidene)ethyl (N-Dde) lipoamino acids. *Molbank* 2008;M566.
3. Schnolzer M, Alewood P, Jones A, Alewood D, Kent SB. *In situ* neutralization in Boc-chemistry solid phase peptide synthesis. Rapid, high yield assembly of difficult sequences. *Int J Pept Protein Res* 1992;**40**:180-93.
4. Palasek SA, Cox ZJ, Collins JM. Limiting racemization and aspartimide formation in microwave-enhanced Fmoc solid phase peptide synthesis. *J Pept Sci* 2007;**13**:143-8.
5. Feng JWA, Kao J, Marshall GR. A second look at mini-protein stability: Analysis of FSD-1 using circular dichroism, differential scanning calorimetry, and simulations. *Biophys J* 2009;**97**:2803-10.
6. Sarin VK, Kent SB, Tam JP, Merrifield RB. Quantitative monitoring of solid-phase peptide synthesis by the ninhydrin reaction. *Anal Biochem* 1981;**117**:147-57.
7. Wu G, Wolf JB, Ibrahim AF, Vadasz S, Gunasinghe M, Freeland SJ. Simplified gene synthesis: A one-step approach to PCR-based gene construction. *J Biotechnol* 2006;**124**:496-503.
8. Brandt ER, Sriprakash KS, Hobb RI, Hayman WA, Zeng W, Batzloff MR, et al. New multi-determinant strategy for a group A streptococcal vaccine designed for the Australian Aboriginal population. *Nat Med* 2000;**6**:455-9.
9. Hayman WA, Brandt ER, Relf WA, Cooper J, Saul A, Good MF. Mapping the minimal murine T cell and B cell epitopes within a peptide vaccine candidate from the conserved region of the M protein of group A streptococcus. *Int Immunol* 1997;**9**:1723-33.
10. Alexander J, Sidney J, Southwood S, Ruppert J, Oseroff C, Maewal A, et al. Development of high potency universal DR-restricted helper epitopes by modification of high affinity DR-blocking peptides. *Immunity* 1994;**1**:751-61.
11. Bryksin AV, Matsumura I. Overlap extension PCR cloning: a simple and reliable way to create recombinant plasmids. *BioTechniques* 2010;**48**:463-5.
12. Tyagarajan K, Pretzer E, Wiktorowicz JE. Thiol-reactive dyes for fluorescence labeling of proteomic samples. *Electrophoresis* 2003;**24**:2348-58.
13. Shafer DE, Inman JK, Lees A. Reaction of Tris(2-carboxyethyl)phosphine (TCEP) with maleimide and alpha-haloacyl groups: anomalous elution of TCEP by gel filtration. *Anal Biochem* 2000;**282**:161-4.
14. Ben-Bassat A, Bauer K, Chang SY, Myambo K, Boosman A, Chang S. Processing of the initiation methionine from proteins: properties of the *Escherichia coli* methionine aminopeptidase and its gene structure. *J Bacteriol* 1987;**169**:751-7.
15. Chandu D, Nandi D. PepN is the major aminopeptidase in *Escherichia coli*: insights on substrate specificity and role during sodium-salicylate-induced stress. *Microbiology* 2003;**149**:3437-47.

16. Brandt ER, Teh T, Relf WA, Hobb RI, Good MF. Protective and nonprotective epitopes from amino termini of M proteins from Australian aboriginal isolates and reference strains of group A streptococci. *Infect Immun* 2000;**68**:6587-94.
17. Batzloff MR, Yan H, Davies MR, Hartas J, Lowell GH, White G, et al. Toward the development of an antidisease, transmission-blocking intranasal vaccine for group A streptococcus. *J Infect Dis* 2005;**192**:1450-5.
18. Pruksakorn S, Galbraith A, Houghten RA, Good MF. Conserved T and B cell epitopes on the M protein of group A streptococci. Induction of bactericidal antibodies. *J Immunol* 1992;**149**:2729-35.
19. Henningham A, Chiarot E, Gillen CM, Cole JN, Rohde M, Fulde M, et al. Conserved anchorless surface proteins as group A streptococcal vaccine candidates. *J Mol Med* 2012;**90**:1197-207.
20. Bauer MJ, Georgousakis MM, Vu T, Henningham A, Hofmann A, Rettel M, et al. Evaluation of novel *Streptococcus pyogenes* vaccine candidates incorporating multiple conserved sequences from the C-repeat region of the M-protein. *Vaccine* 2012;**30**:2197-205.